Electronic Supplementary Material (ESI) for Dalton Transactions.
This journal is © The Royal Society of Chemistry 2023

Energy transfer in metal-exchange binuclear complexes covalently linked by asymmetric ligands

Weijun Dai, Shiwen Yu, Wen Xu, Ci Kong, Zining Liu, Hongju Yin, Chixian He, Jian-Jun Liu*, Feixiang Cheng*

College of Chemistry and Environmental Science, Qujing Normal University, Qujing 655011

E-mail: jjliu302@163.com; chengfx2019@163.com

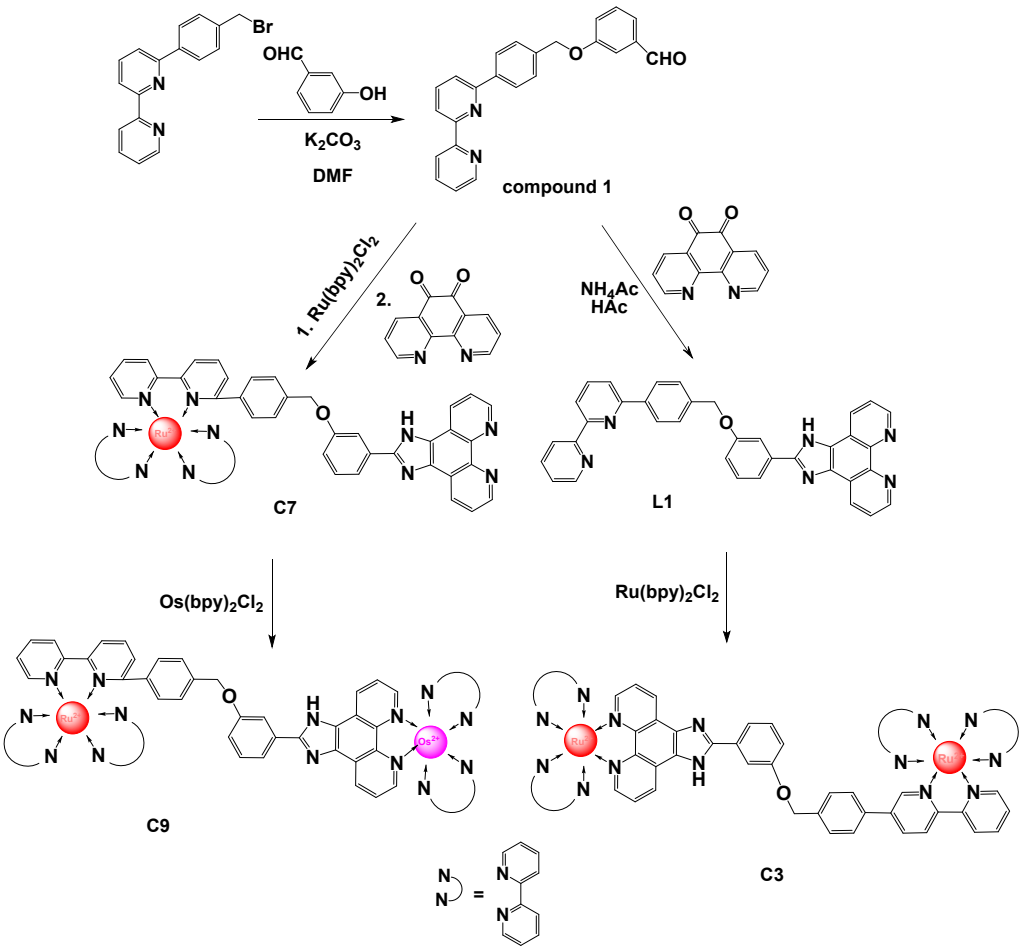

Scheme S1. Chemical structures of the target monometallic **C7**, homometallic **C3**, heterometallic **C9** complexes and corresponding bridging ligand **L1**. (The counter ions are omitted for clarity. The same below).

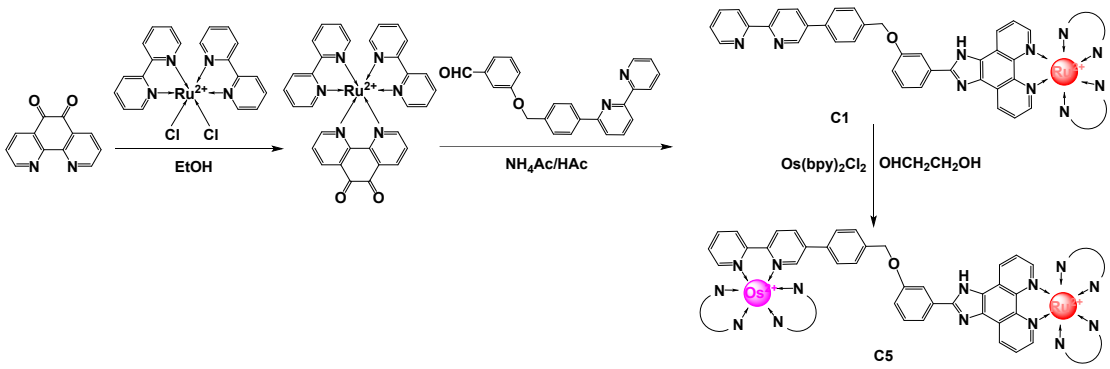

Scheme S2. Chemical structures of the target monometallic **C1**, homometallic **C5** complexes.

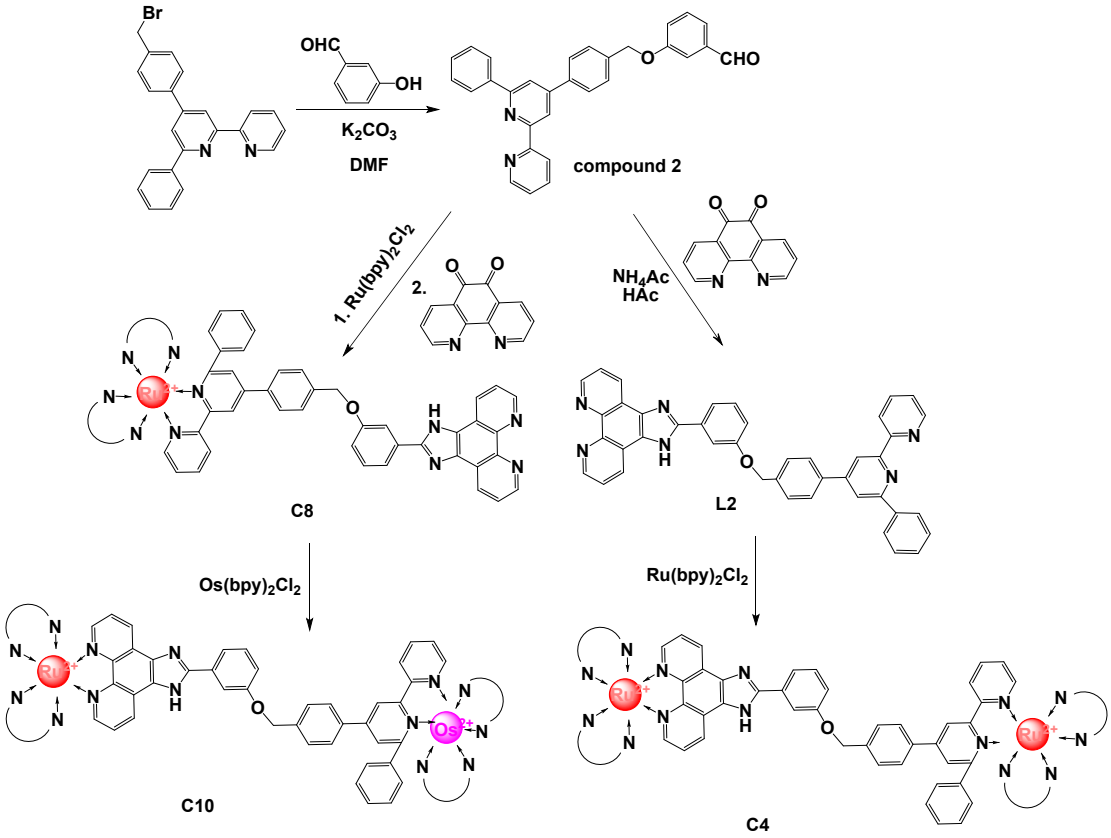

Scheme S3. Chemical structures of the target monometallic complex **C8**, homometallic complexes **C4**, **C10** bridged by ligand **L2**.

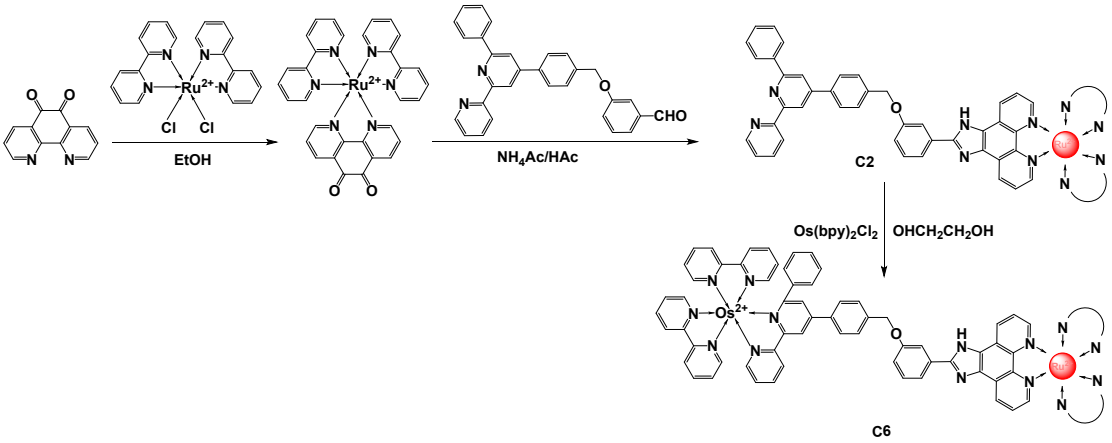

Scheme S4. Chemical structures of the target monometallic complex **C2**, heterometallic complex **C6**.

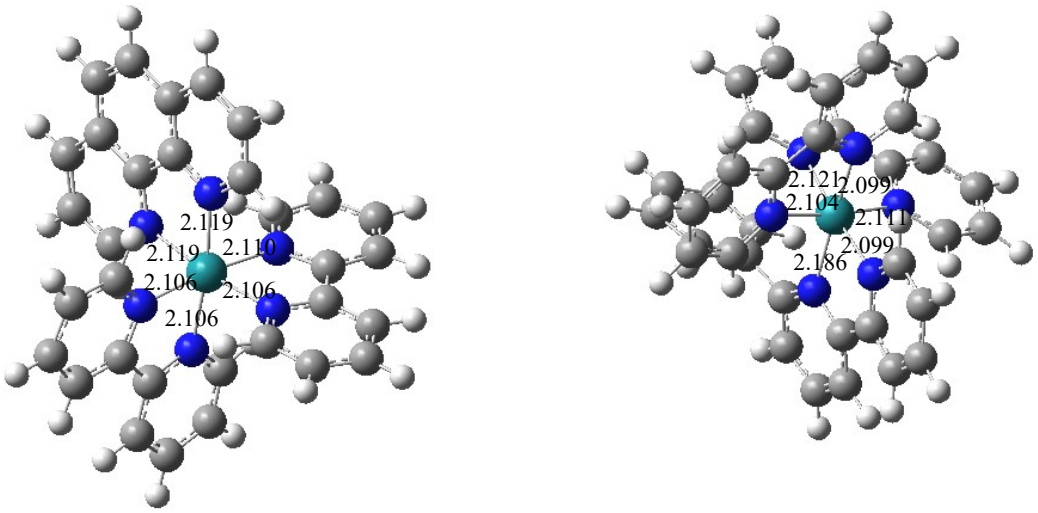

(a) (b)

Scheme S5. The Ru–N bond lengths of octahedral Ru(bpy)$_2$(1,10-phenanthroline) moieties of complex **C4**, **C8** and **C10** presented in (a) and Ru–N bond lengths of the octahedral Ru(bpy)$_2$(6-phenyl-2,2'-bipyridine) of complexes **C2**, **C4** and **C6** presented in (b).

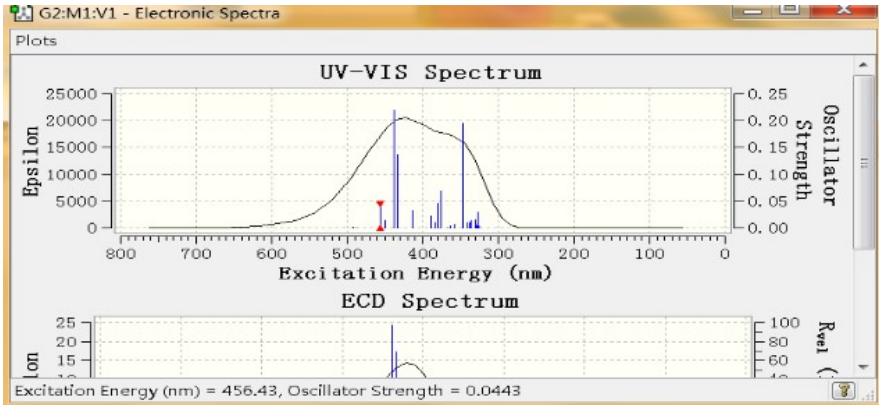

Figure S1. The UV-Vis spectrum of TD-DFT calculation of **C1**.

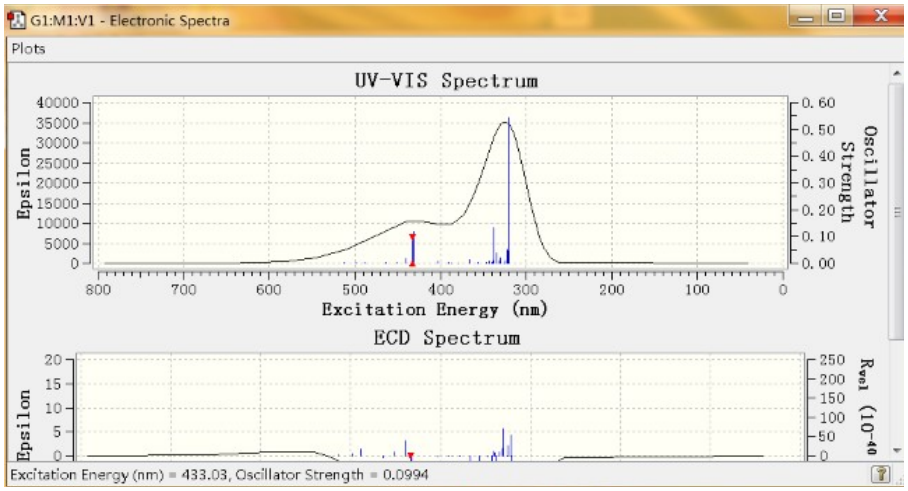

Figure S2. The UV-Vis spectrum of TD-DFT calculation of **C7**.

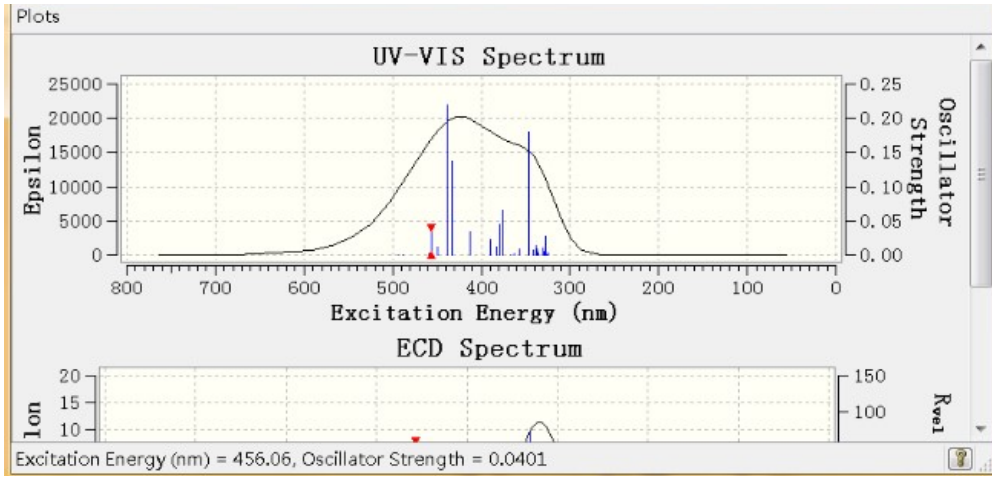

Figure S3. The UV-Vis spectrum of TD-DFT calculation of **C2**.

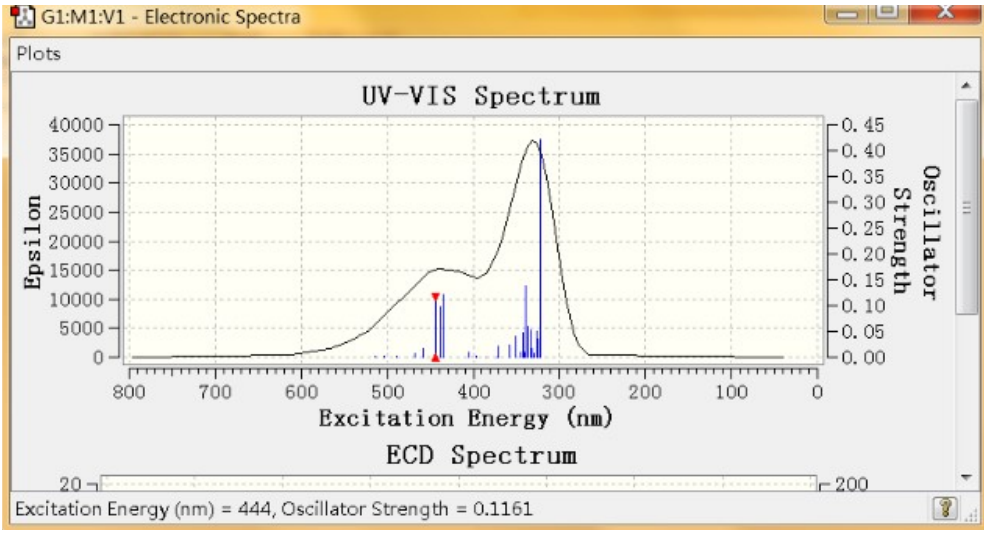

Figure S4. The UV-Vis spectrum of TD-DFT calculation of **C8**.

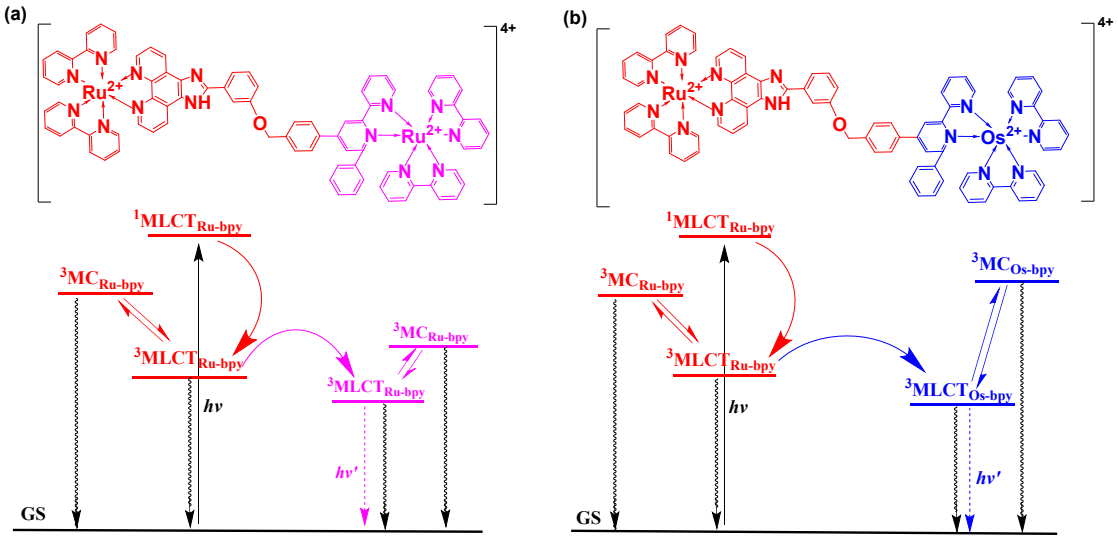

Figure S5. Energy level mechanism of the emissive state of multinuclear complexes **C4** (a), **C6** (b), where the straight line represents excitation; the dotted line represents luminescence, and the wavy line represents radiationless decay.

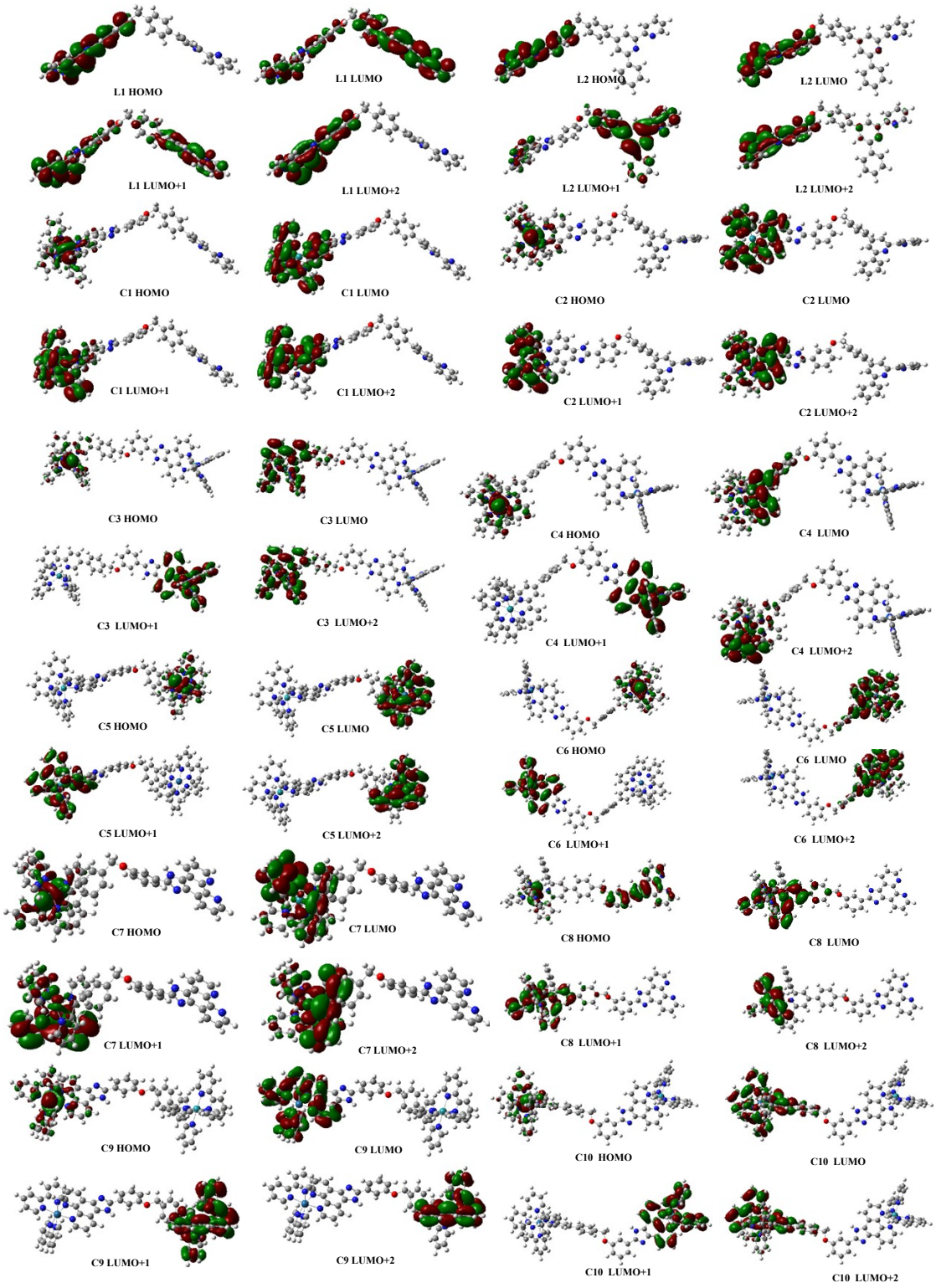

Figure S6. The HOMO and the LUMOs of all complexes.

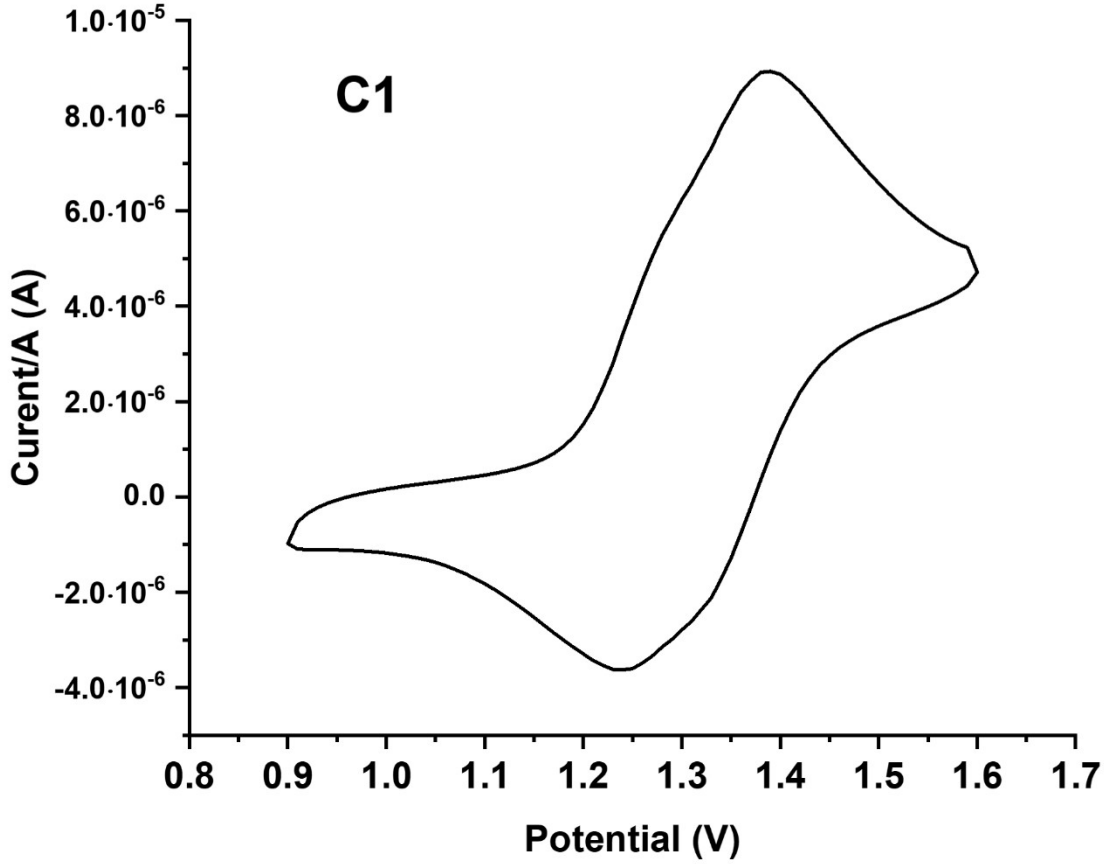

Figure S7. Oxidation cyclic voltammetry of complex **C1**.

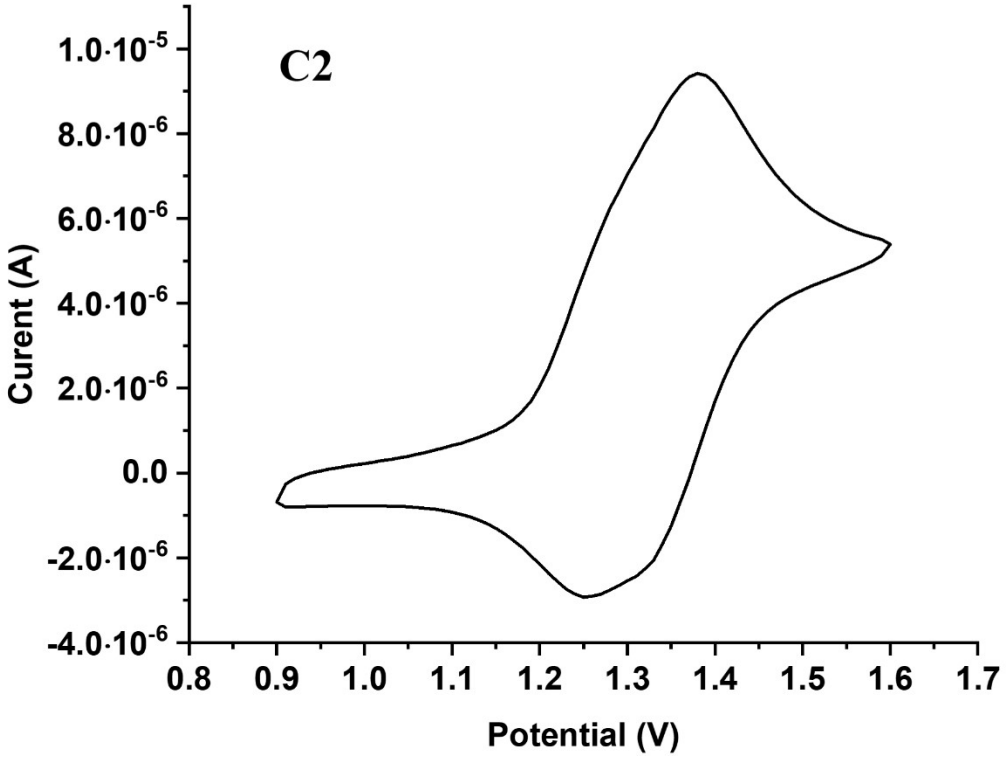

Figure S8. Oxidation cyclic voltammetry of complex **C2**.

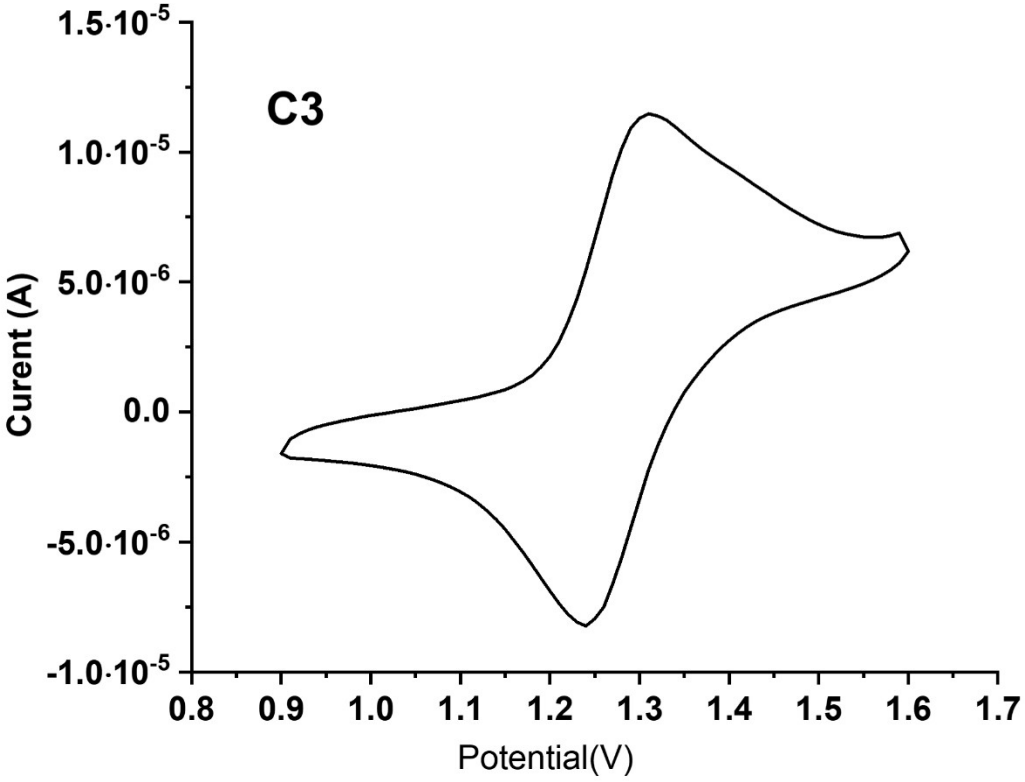

Figure S9. Oxidation cyclic voltammetry of complex **C3**.

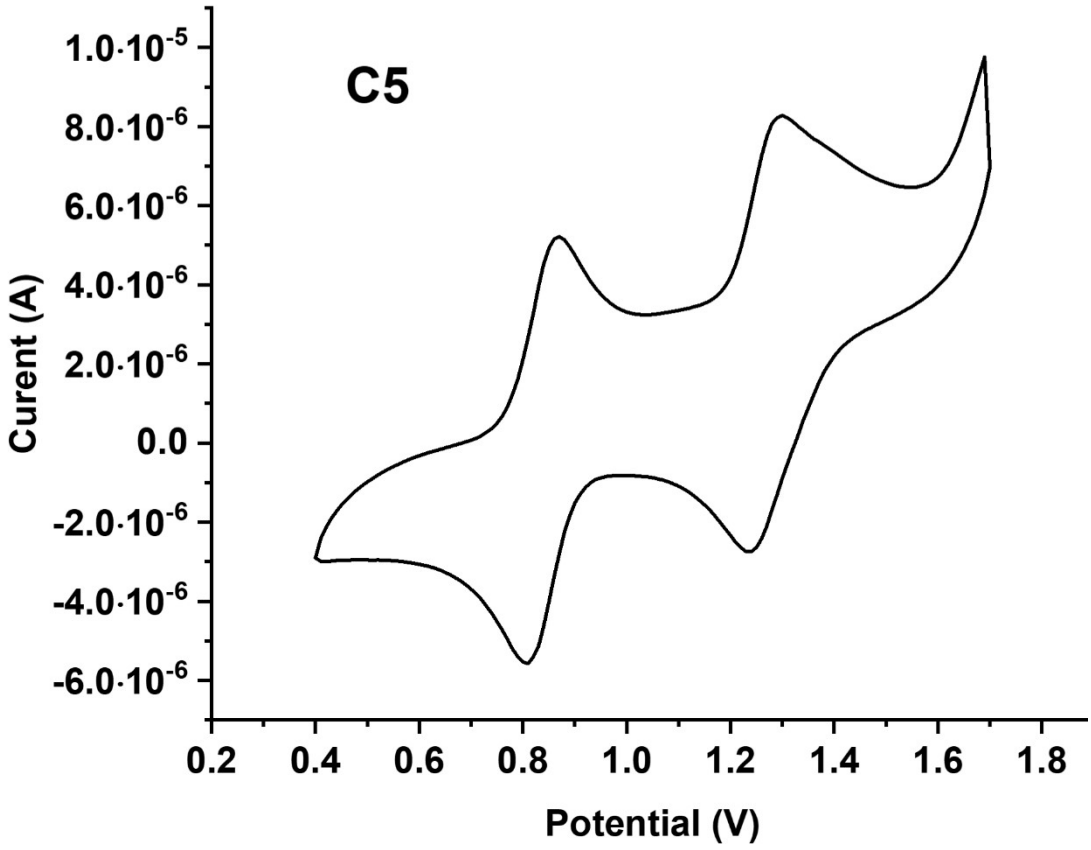

Figure S10. Oxidation cyclic voltammetry of complex **C5**.

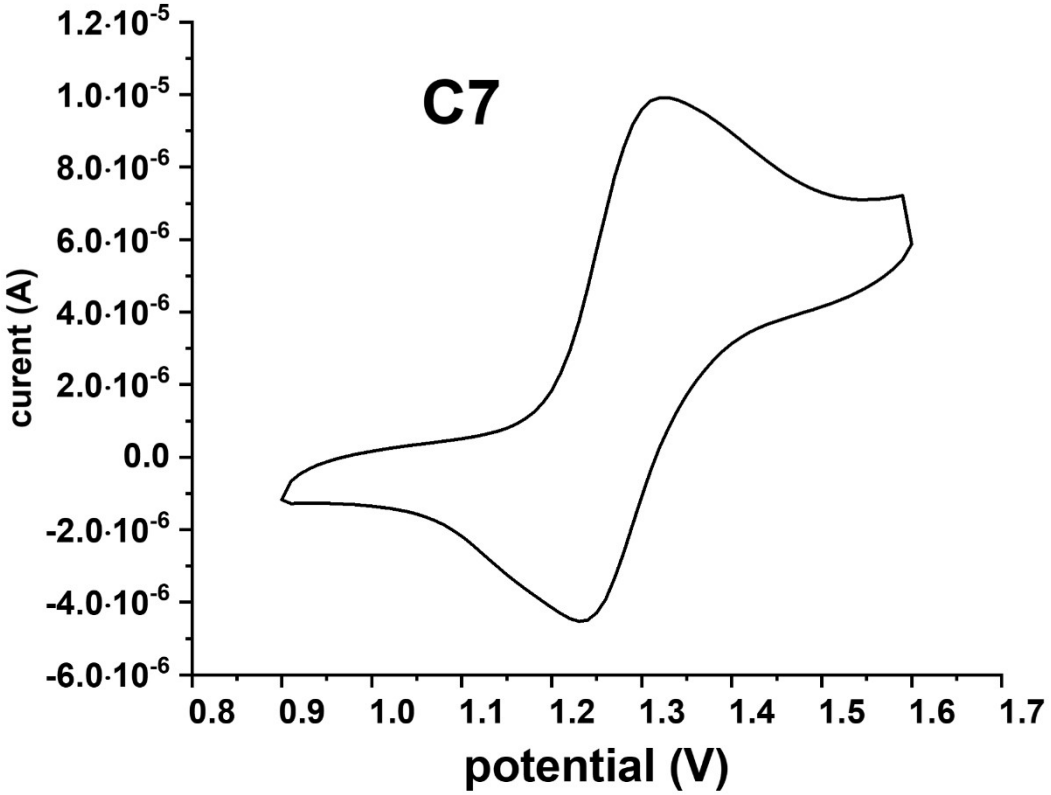

Figure S11. Oxidation cyclic voltammetry of complex **C7**.

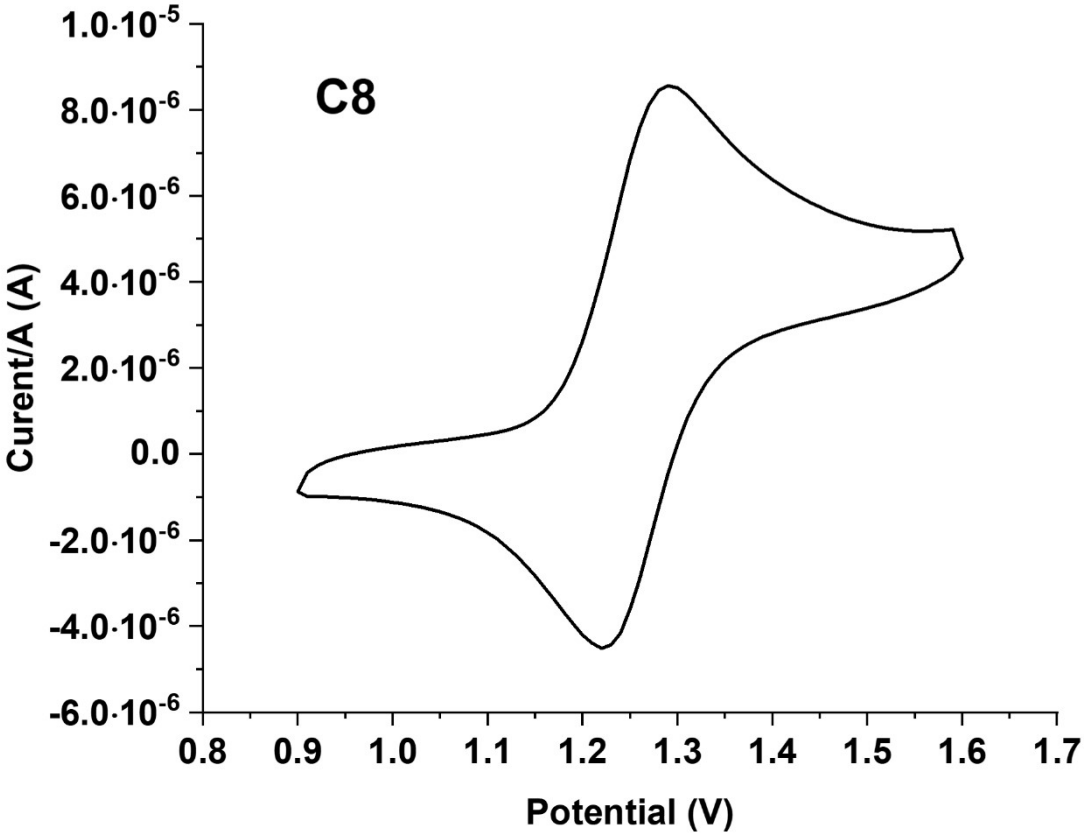

Figure S12. Oxidation cyclic voltammetry of complex **C8**.

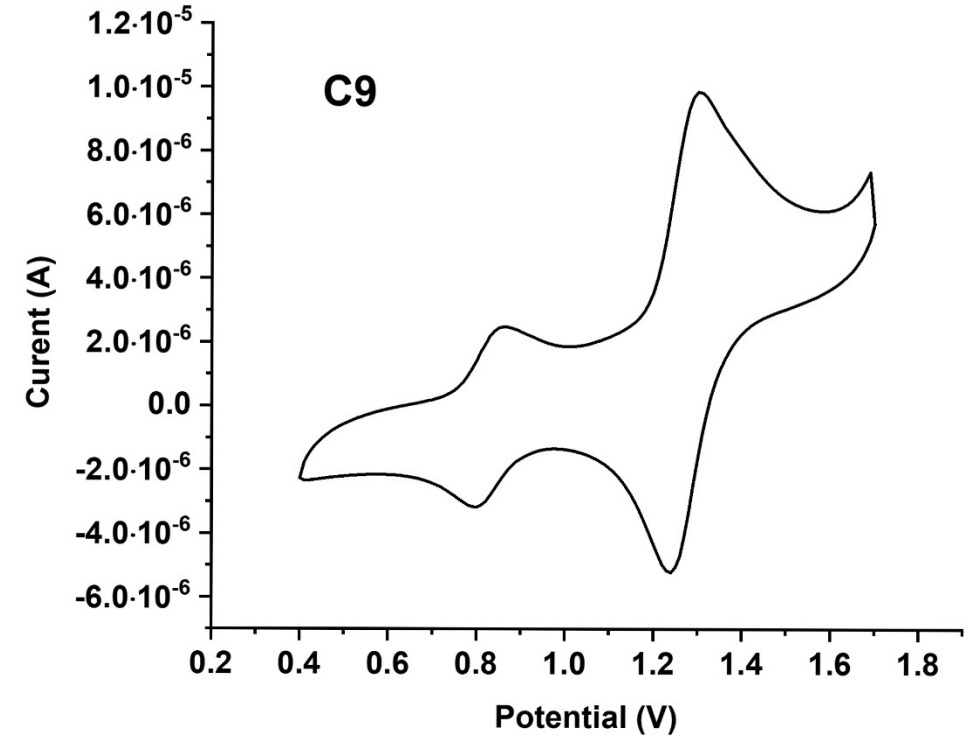

Figure S13. Oxidation cyclic voltammetry of complex **C9**.

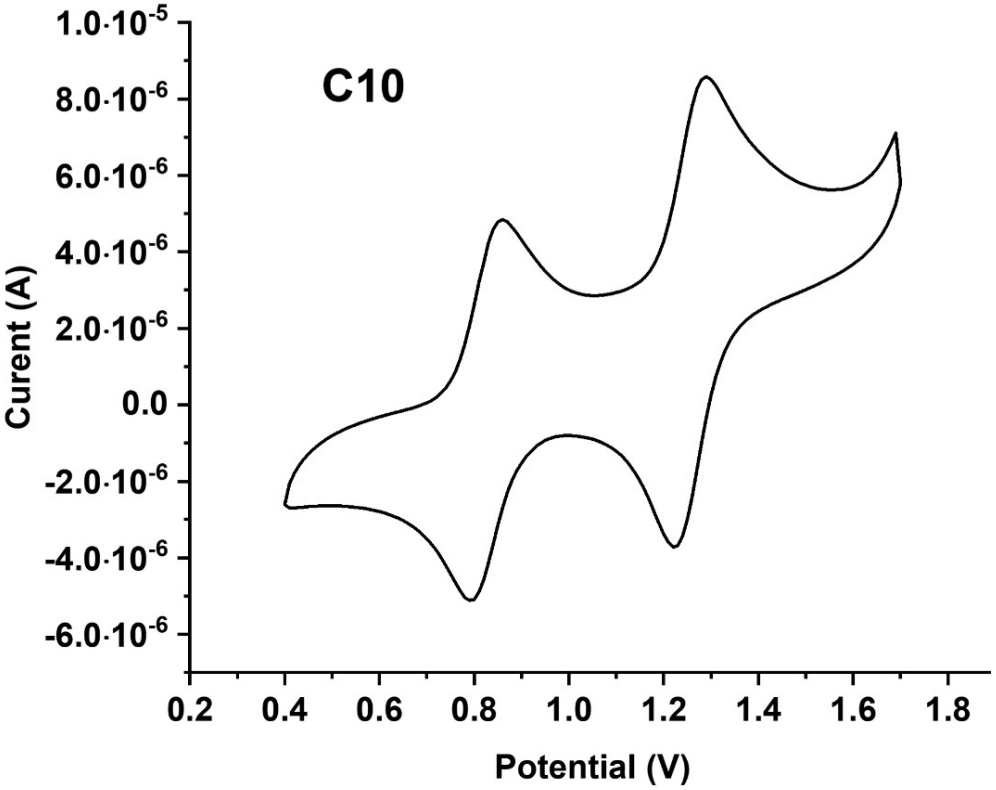

Figure S14. Reduction cyclic voltammetry of complex **C10**.

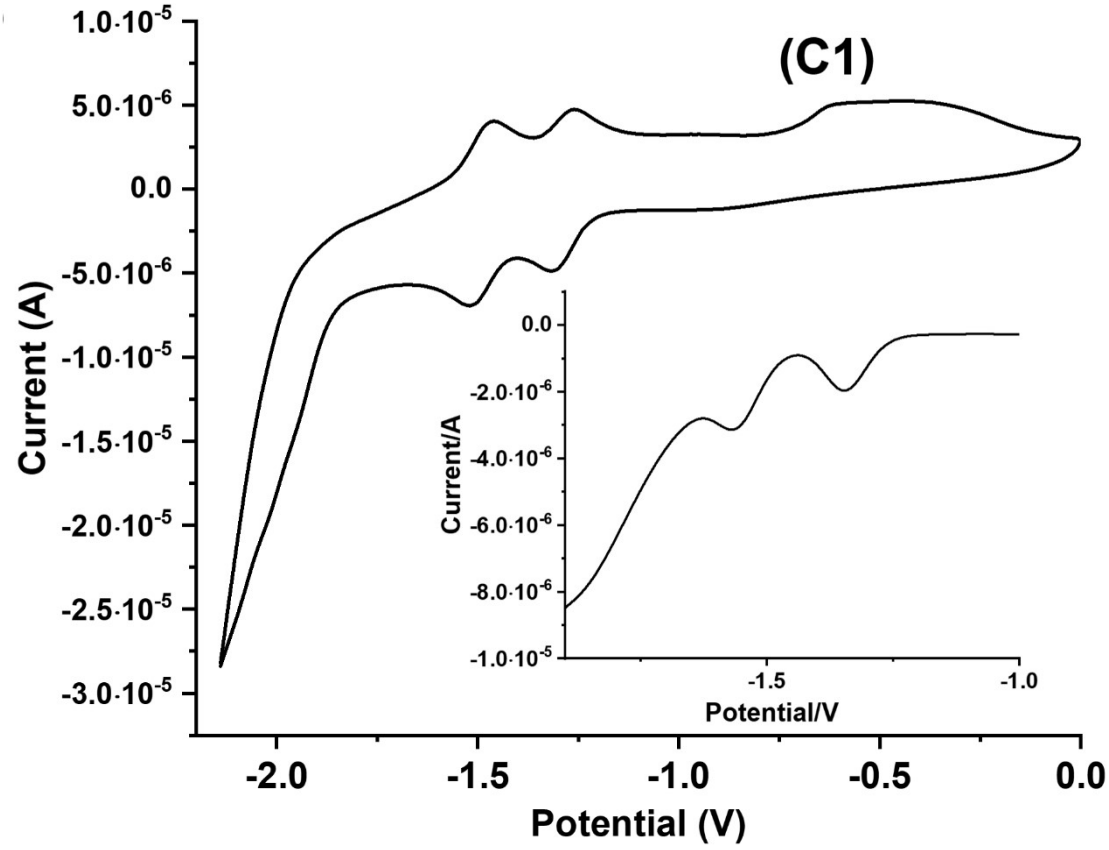

Figure S15. Reduction cyclic voltammetry of complex **C1**.

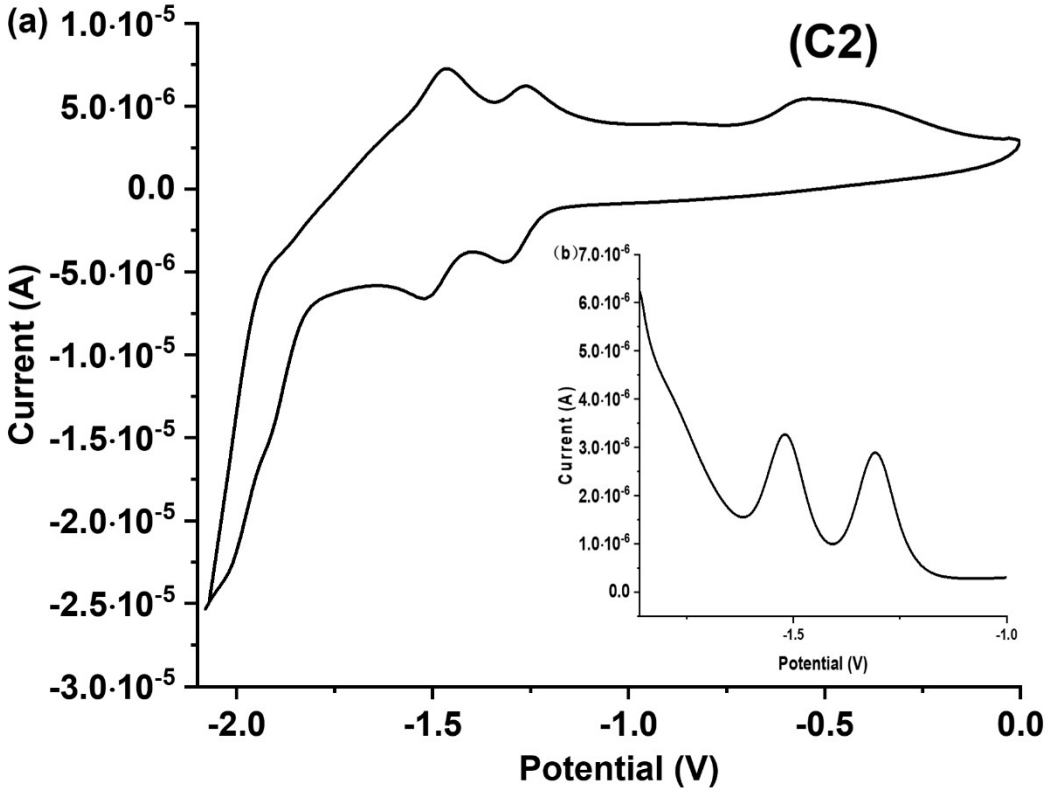

Figure S16. Reduction cyclic voltammetry of complex **C2**.

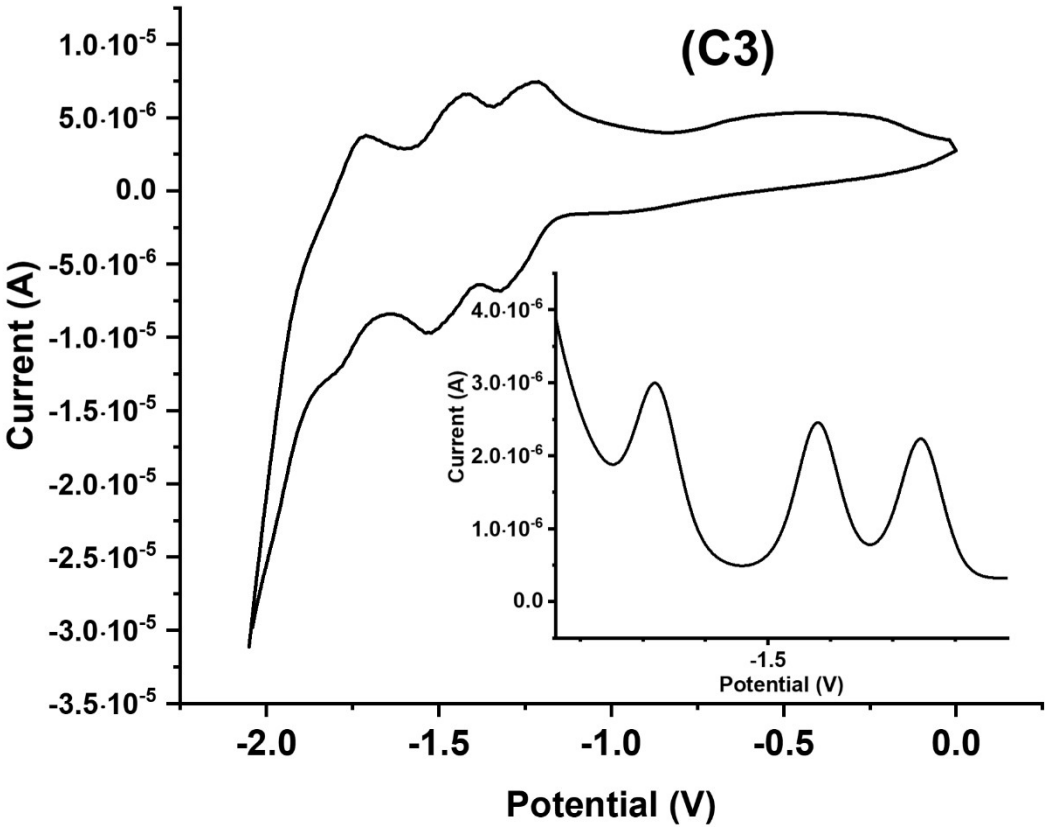

Figure S17. Reduction cyclic voltammetry of complex **C3**.

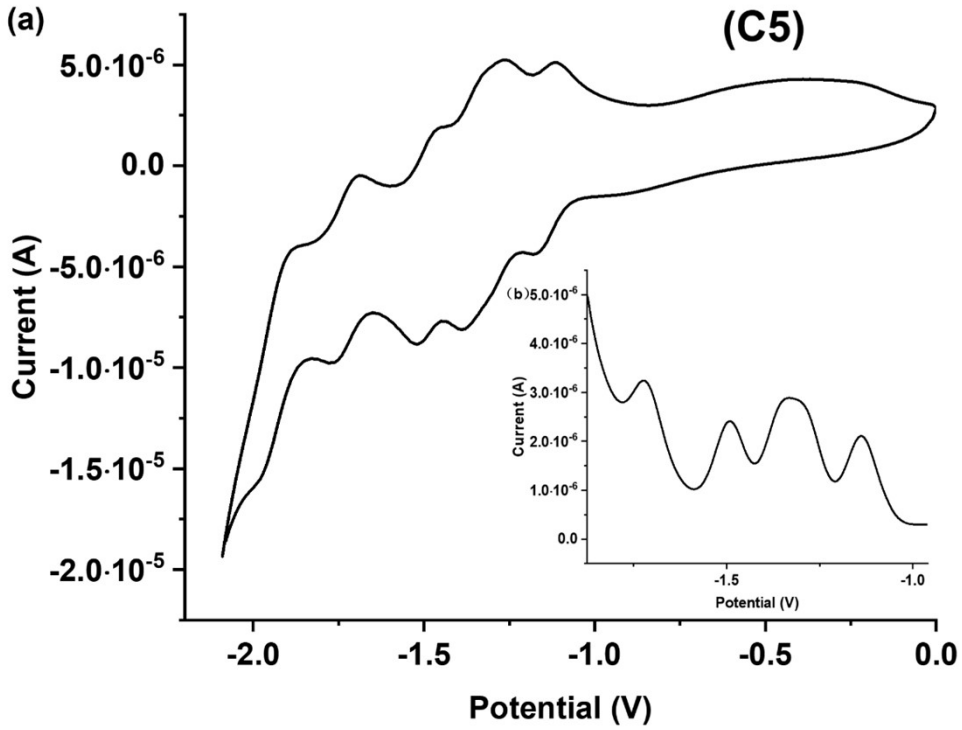

Figure S18. Reduction cyclic voltammetry of complex **C5**.

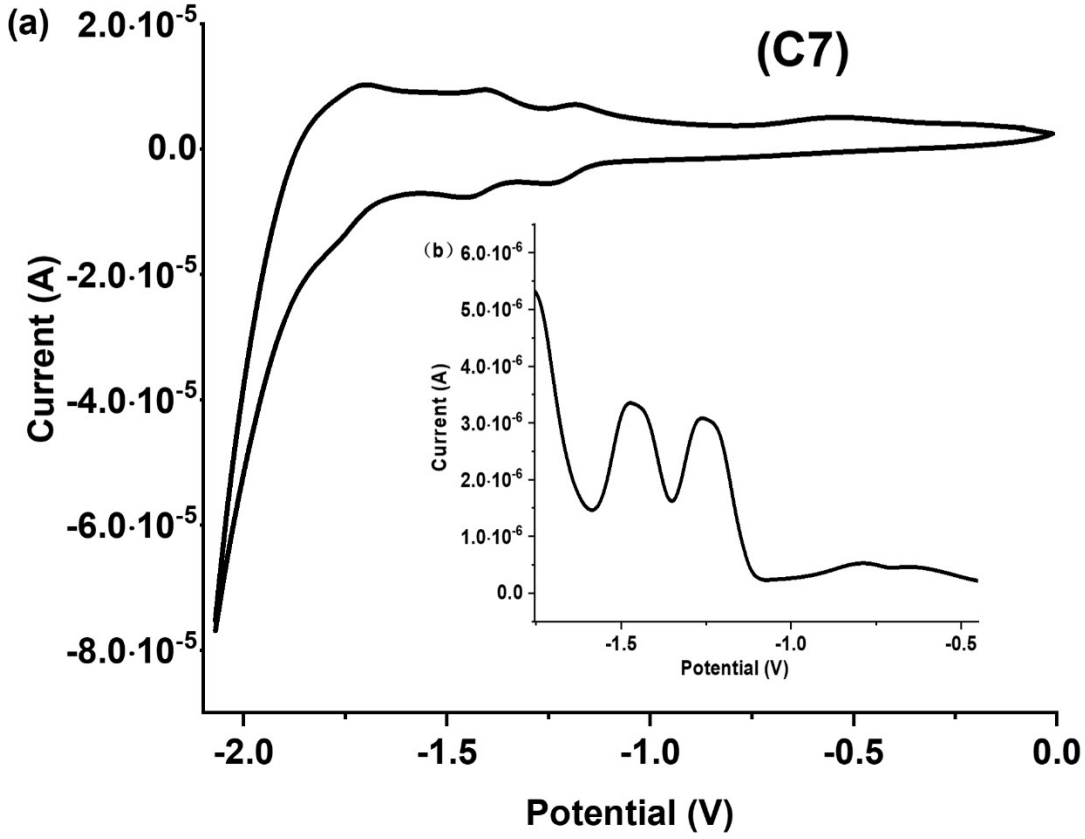

Figure S19. Reduction cyclic voltammetry of complex **C7**.

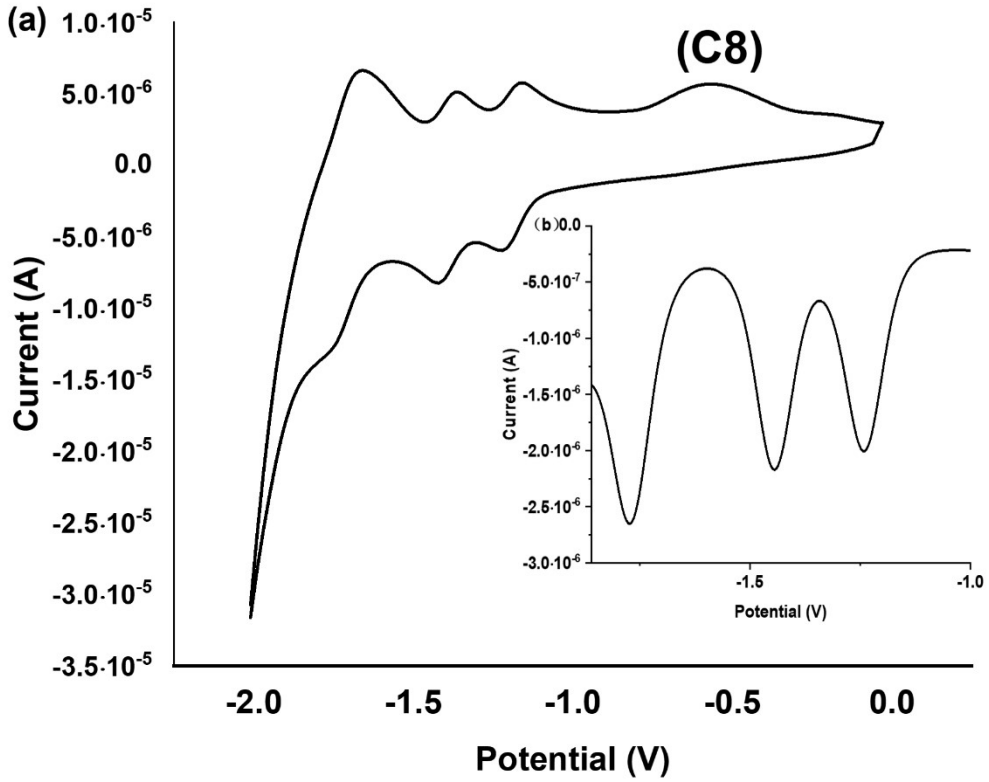

Figure S20. Reduction cyclic voltammetry of complex **C8**.

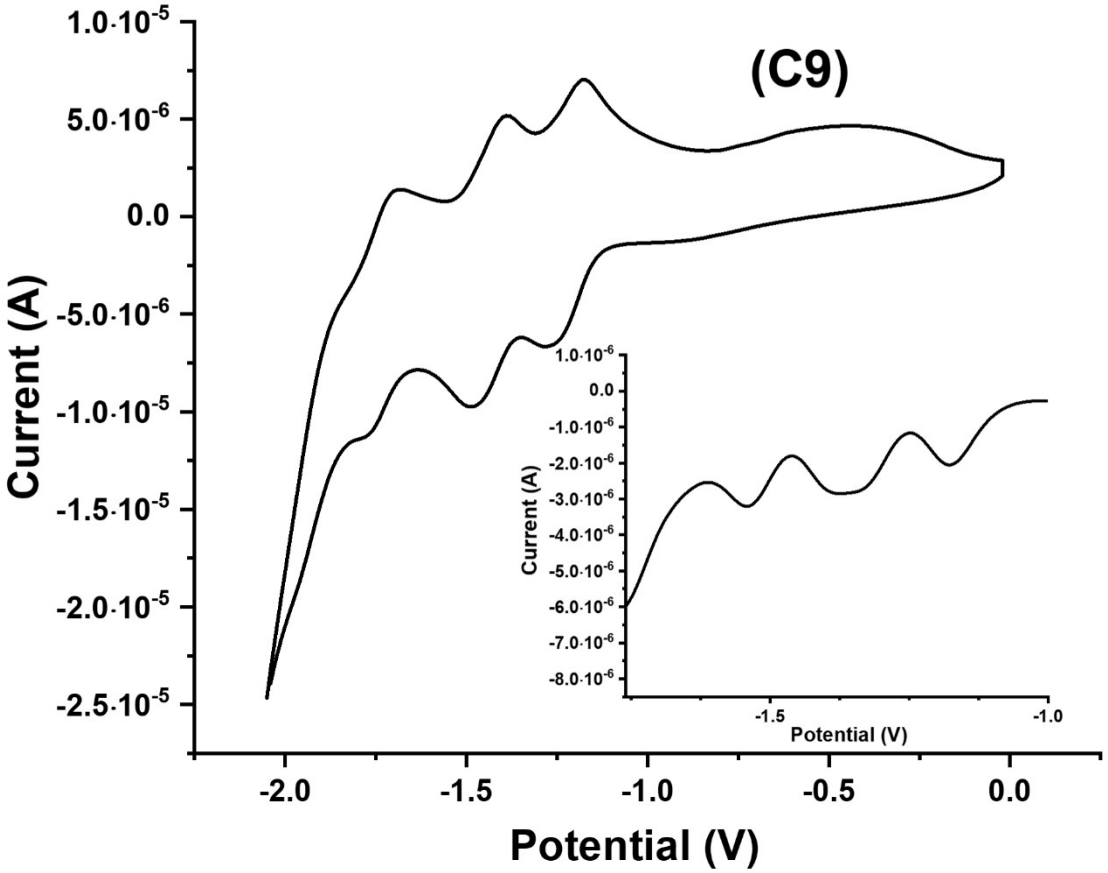

Figure S21. Reduction cyclic voltammetry of complex **C9**.

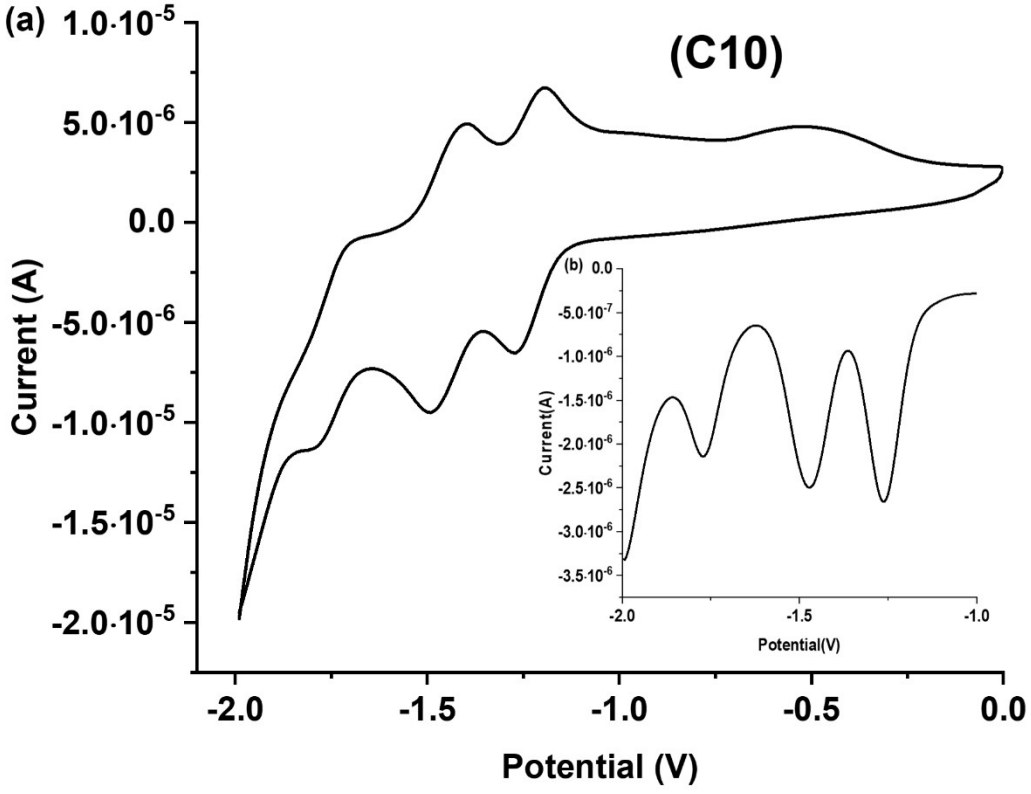

Figure S22. Reduction cyclic voltammetry of complex **C10**.

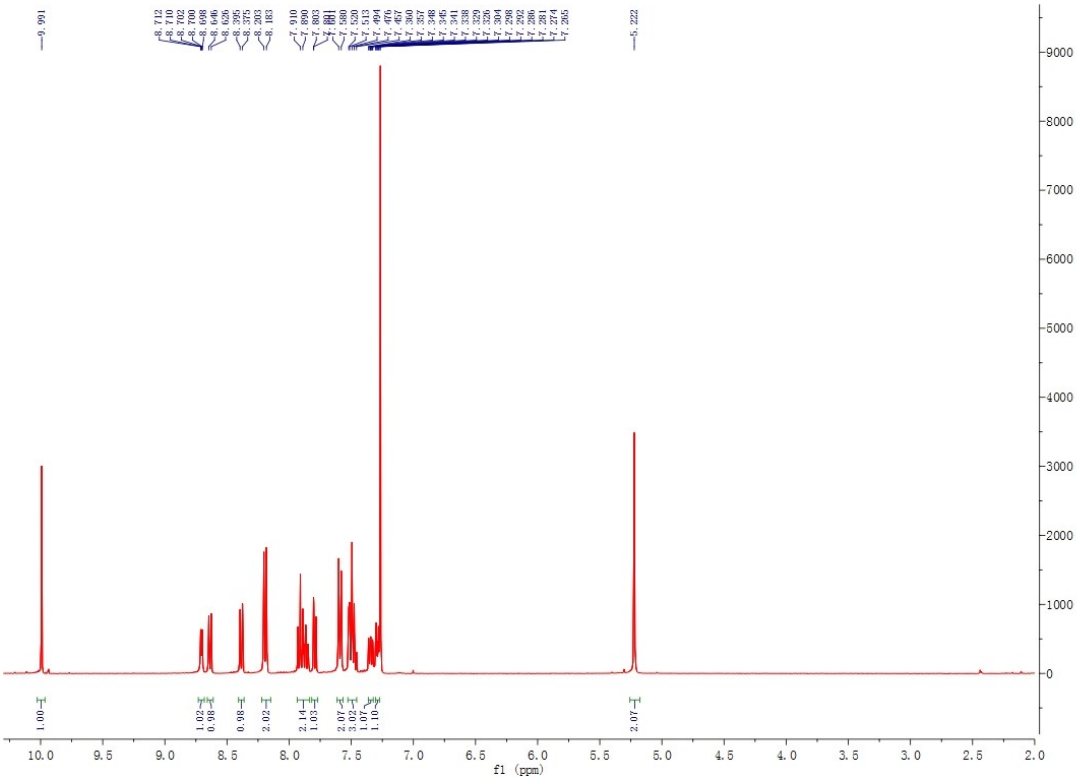

Figure S23. ^{1}H NMR (400 MHz, $CDCl_3$) spectrum of compound 1.

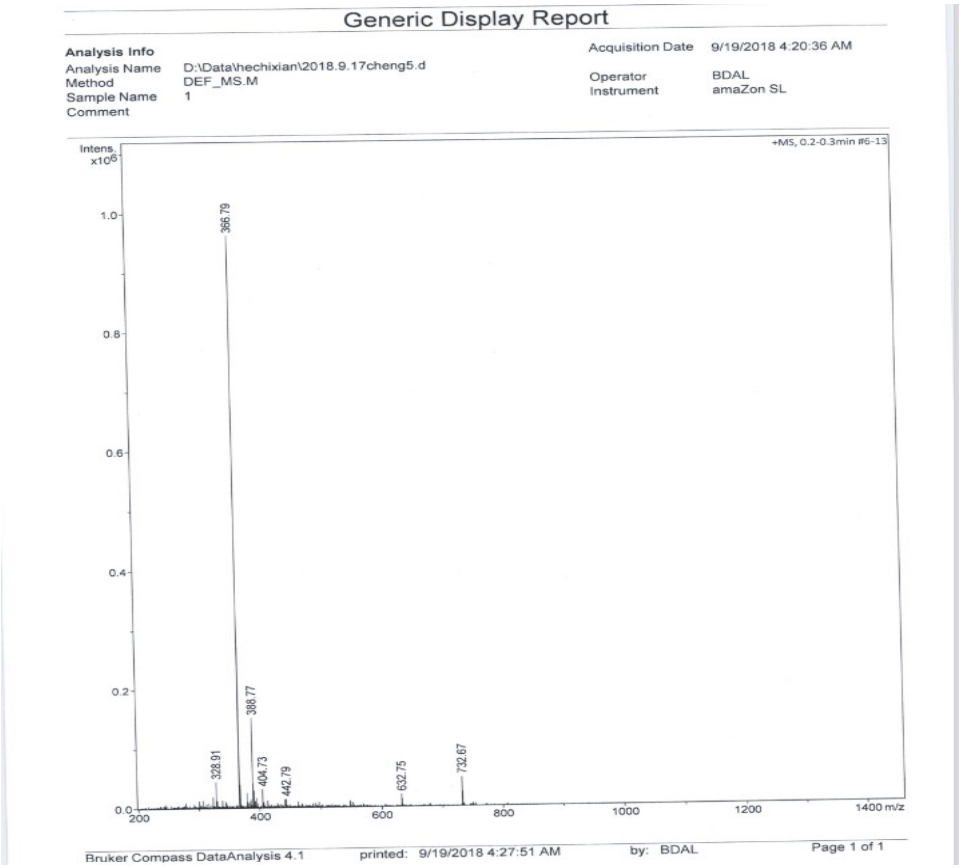

Figure S24. ESI-MS of **compound 1**.

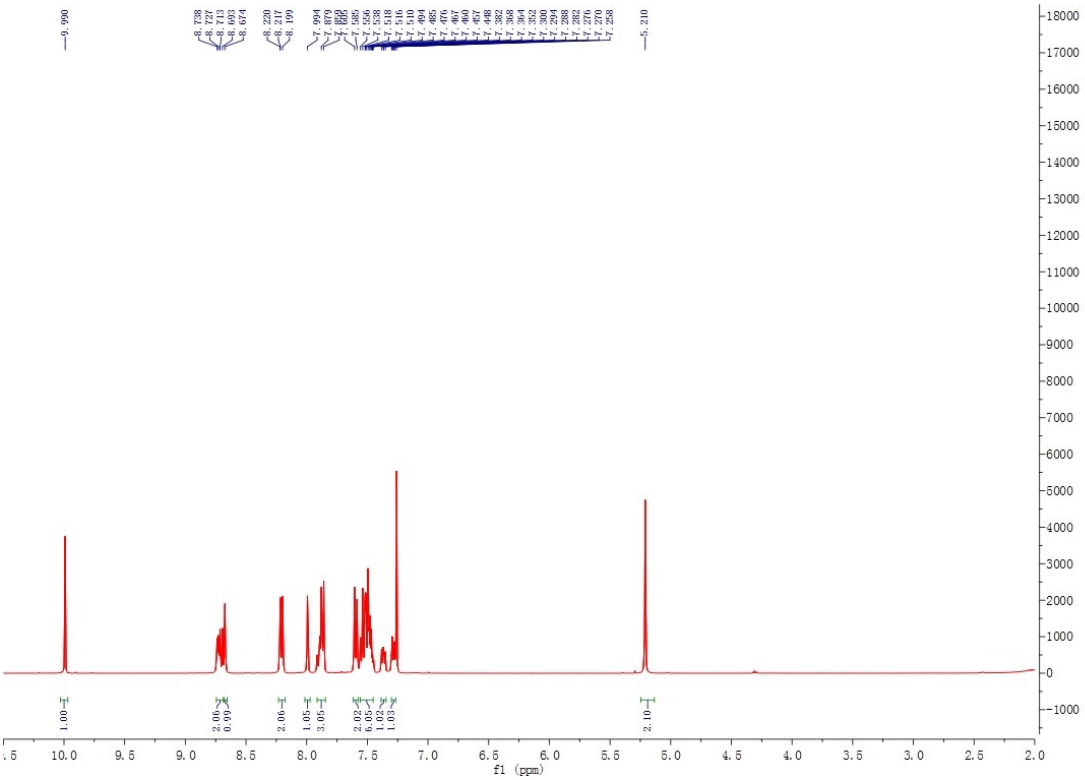

Figure S25. ^{1}H NMR (400 MHz, $CDCl_3$) spectrum of **compound 2.**

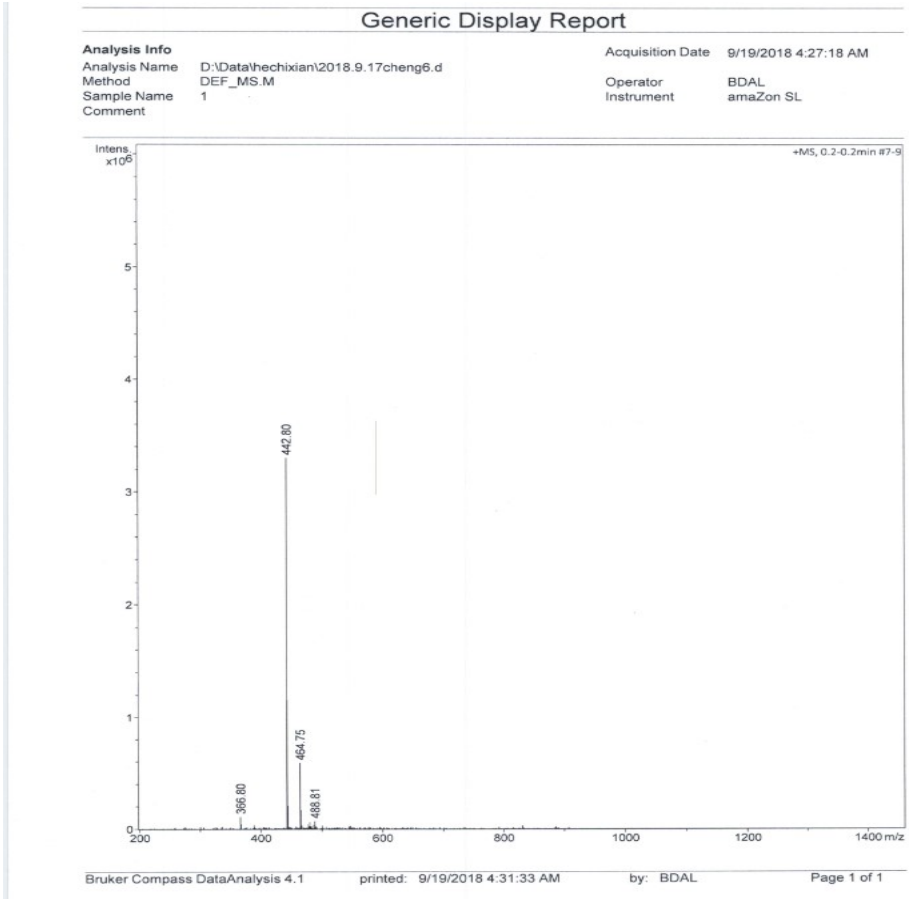

Figure S26. ESI-MS of **compound 2**.

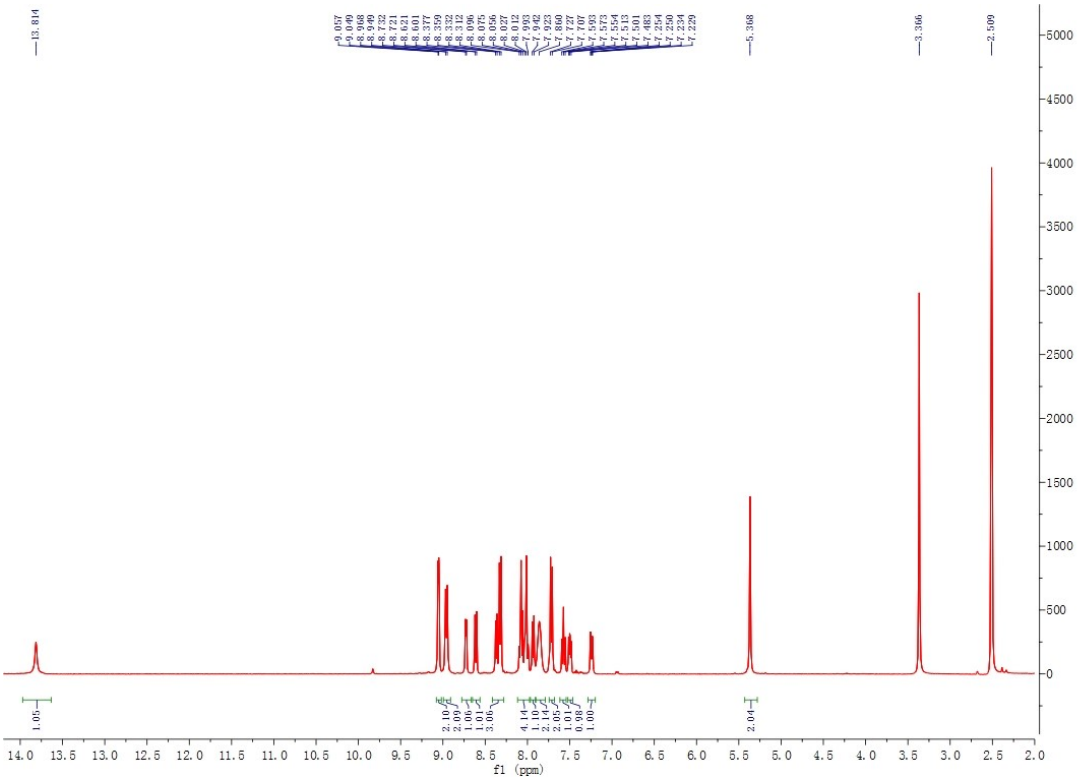

Figure S27. ^{1}H NMR (400 MHz, DMSO-d_6) spectrum of ligand **L1**.

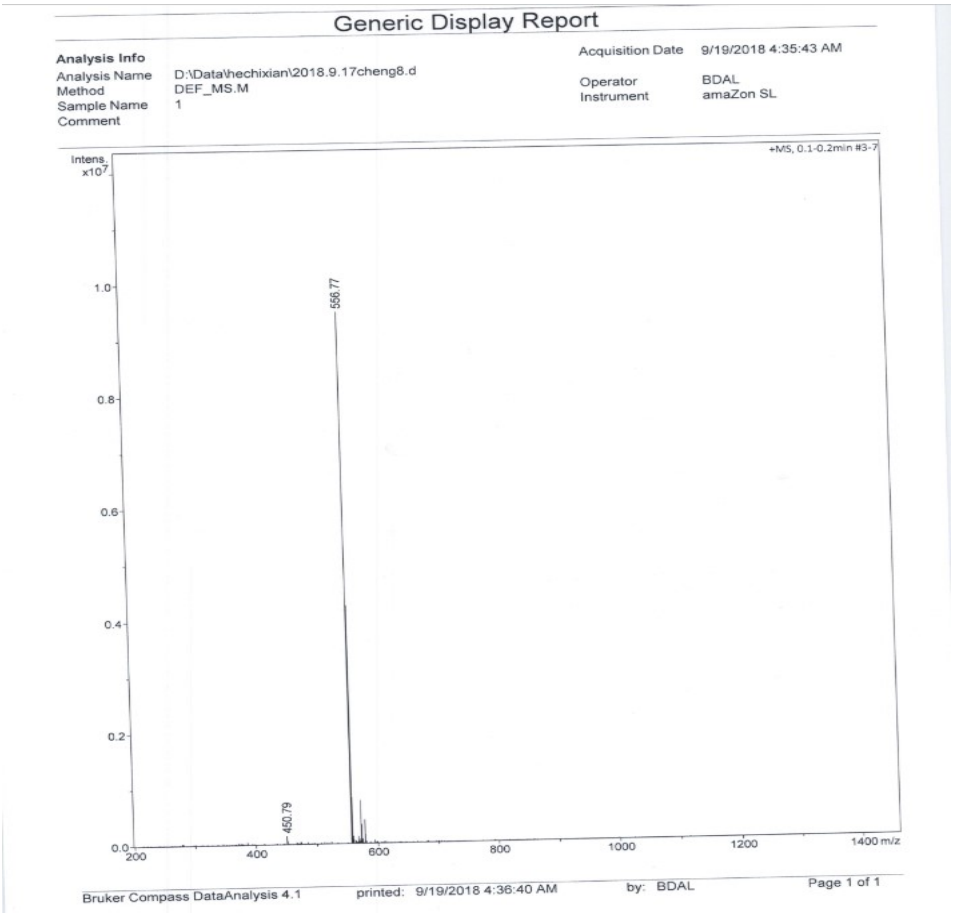

Figure S28. ESI-MS of ligand **L1**.

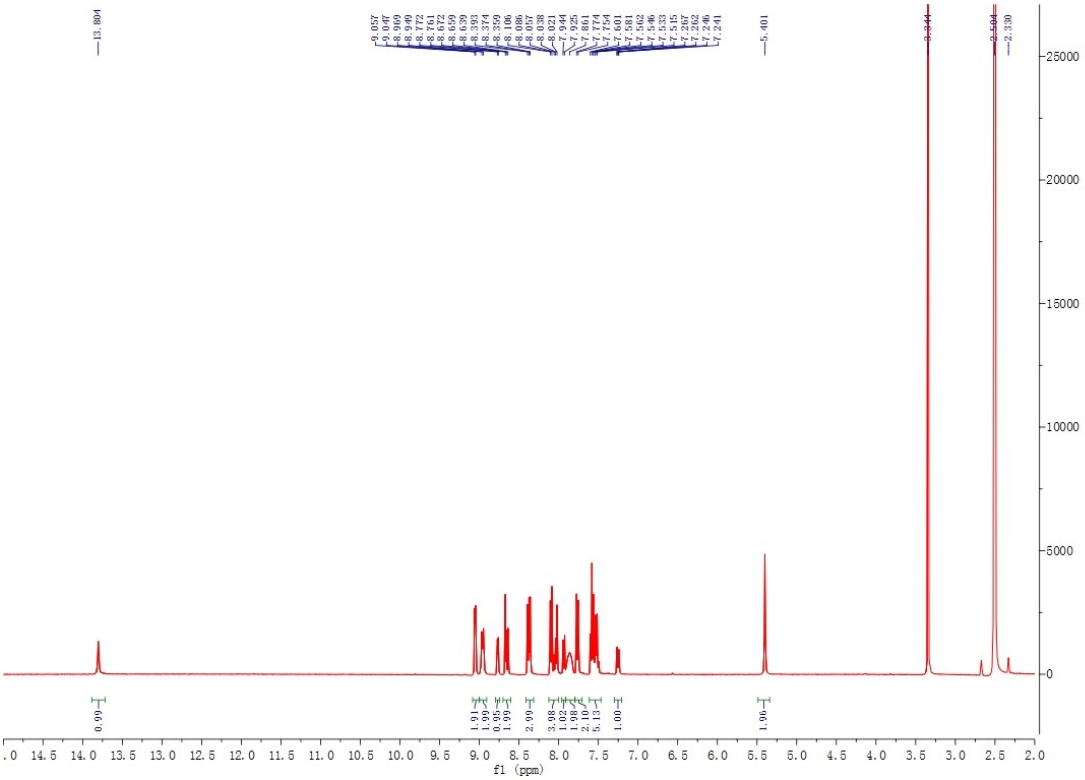

Figure S29. ^{1}H NMR (400 MHz, DMSO-d_6) spectrum of ligand **L2**.

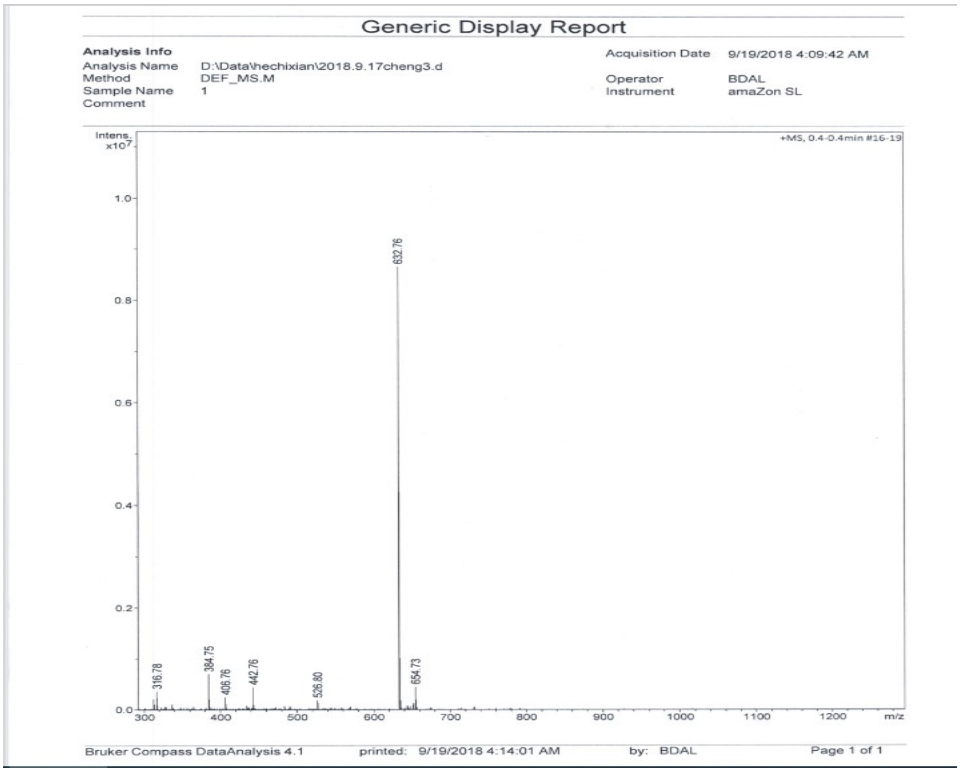

Figure S30. ESI-MS of ligand **L2**.

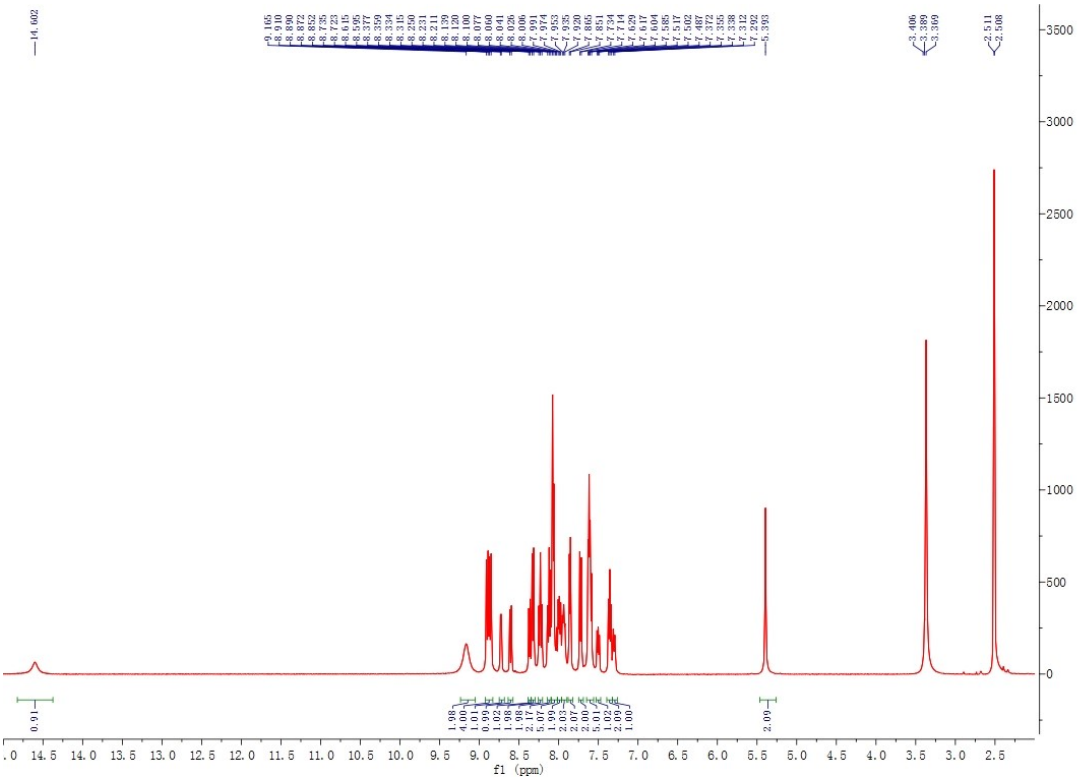

Figure S31. ^{1}H NMR (400 MHz, DMSO-d_6) spectrum of complex **C1**.

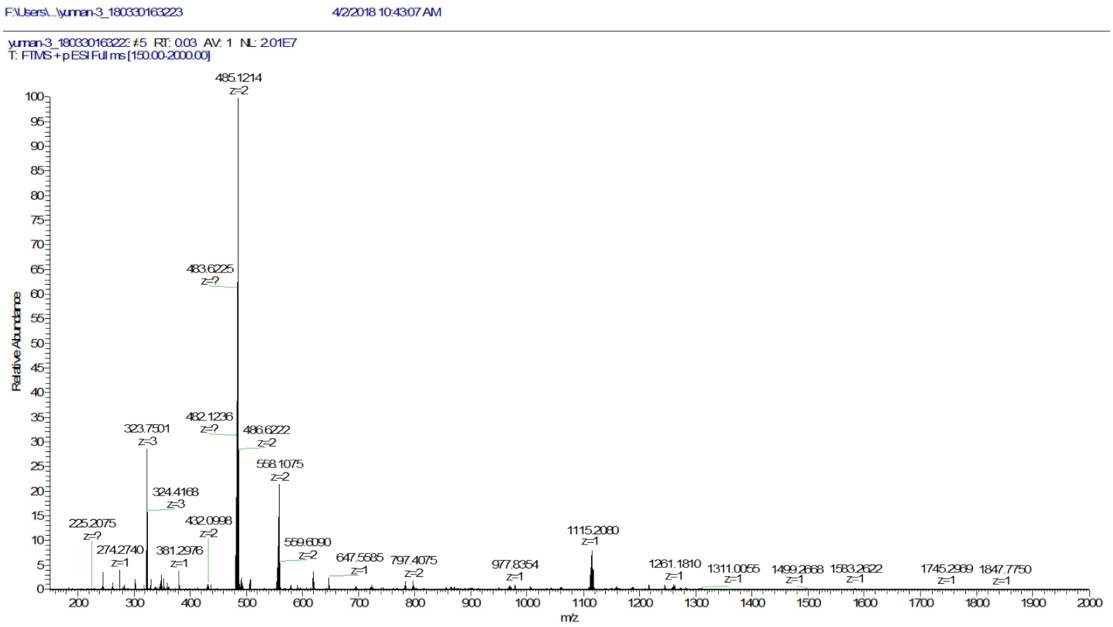

Figure S32. ESI-HRMS of complex **C1**.

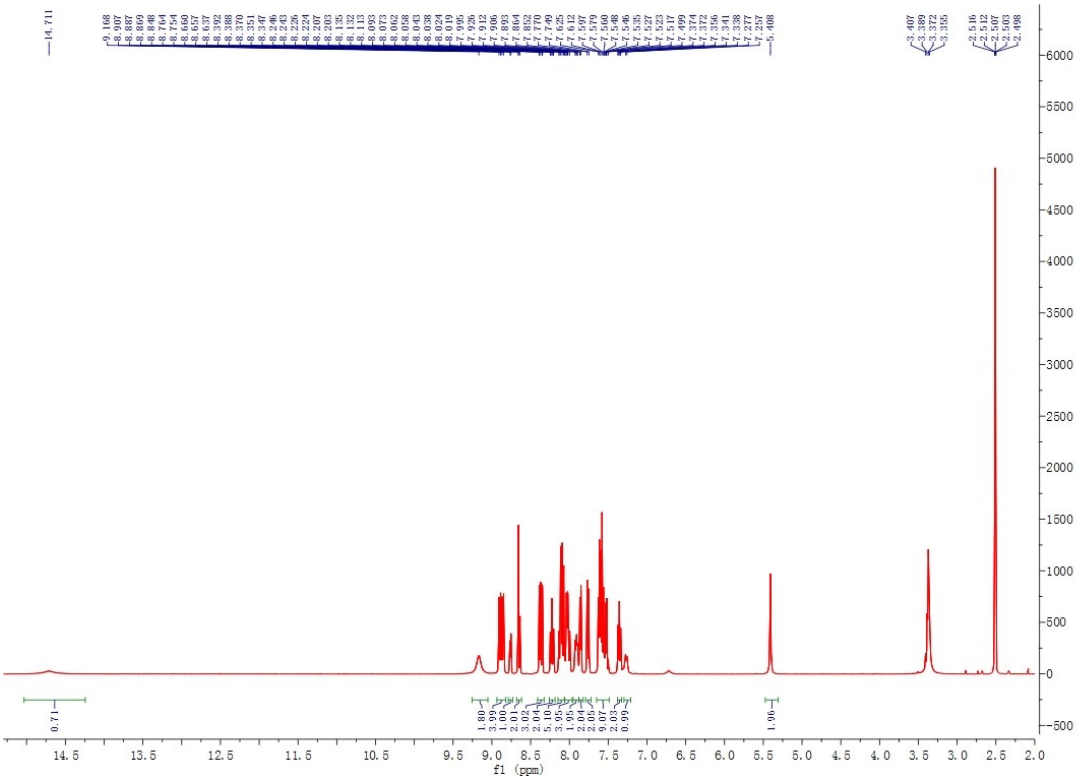

Figure S33. ^{1}H NMR (400 MHz, DMSO-d_6) spectrum of complex **C2**.

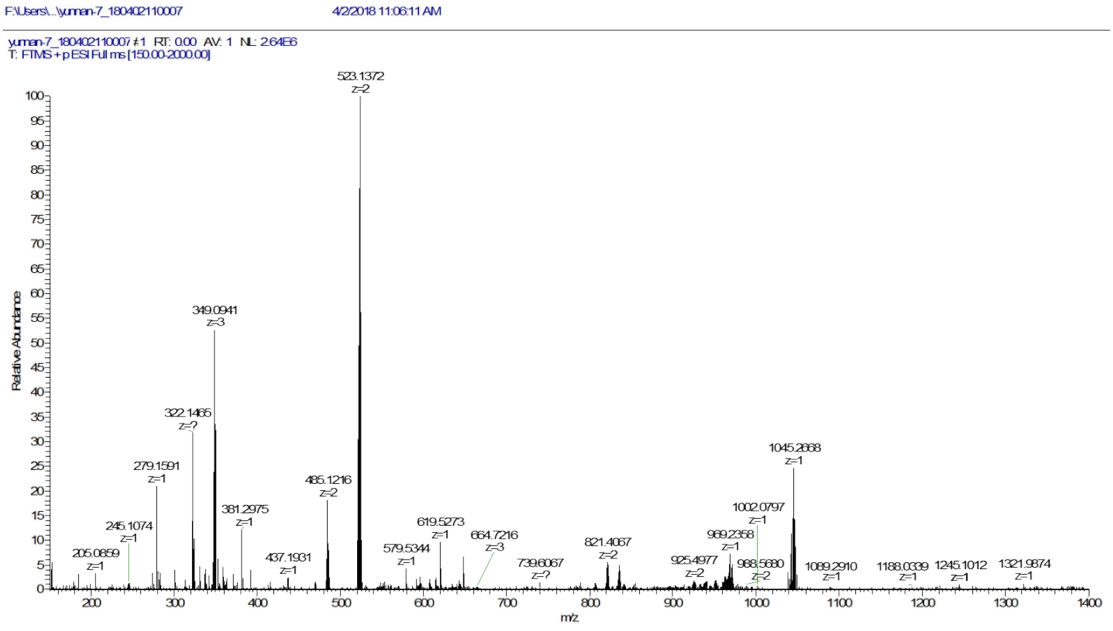

Figure S34. ESI-HRMS of complex **C2**.

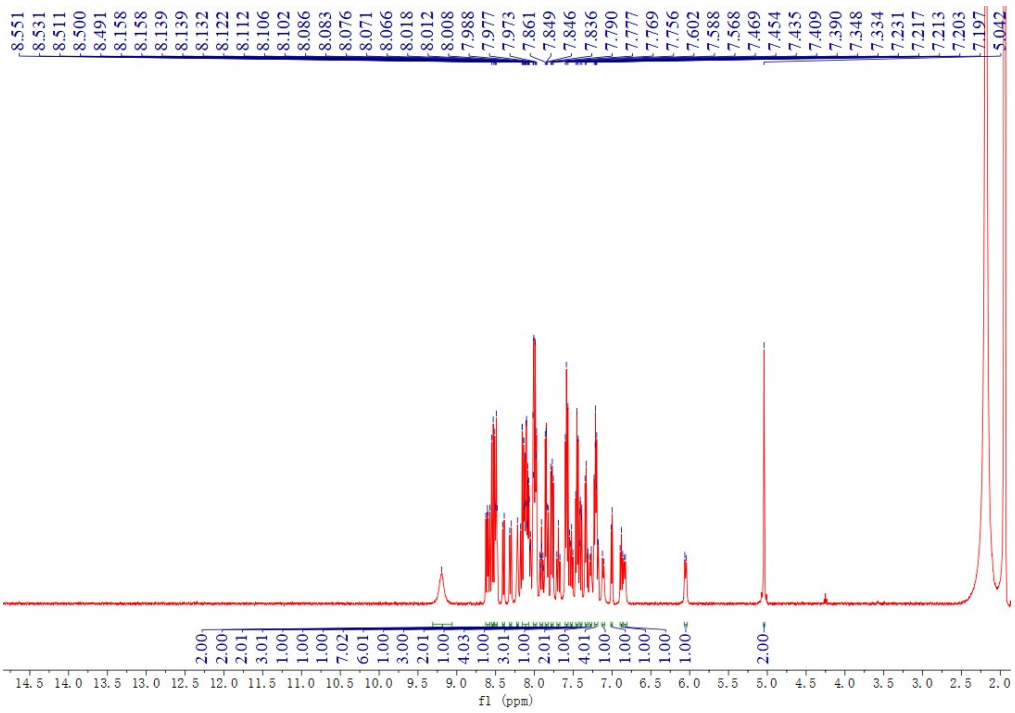

Figure S35. ^{1}H NMR (400 MHz, MeCN-d_3) spectrum of complex **C3**.

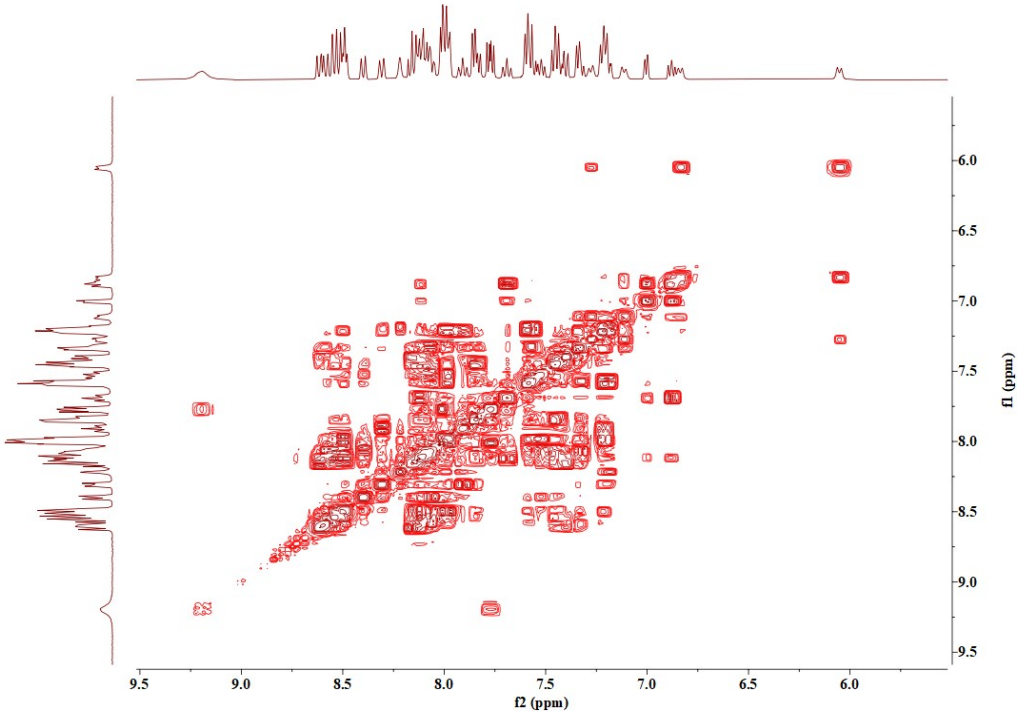

Figure S36. ^{1}H-^{1}H COSY (400 MHz, MeCN-d_3) spectrum of complex **C3**.

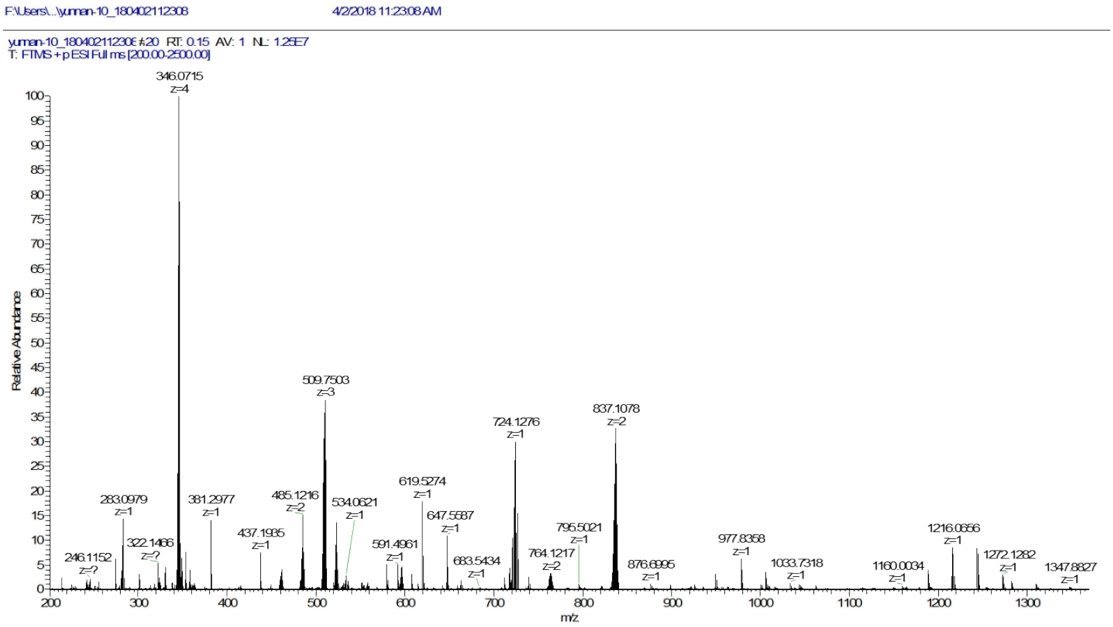

Figure S37. ESI-HRMS of complex **C3**.

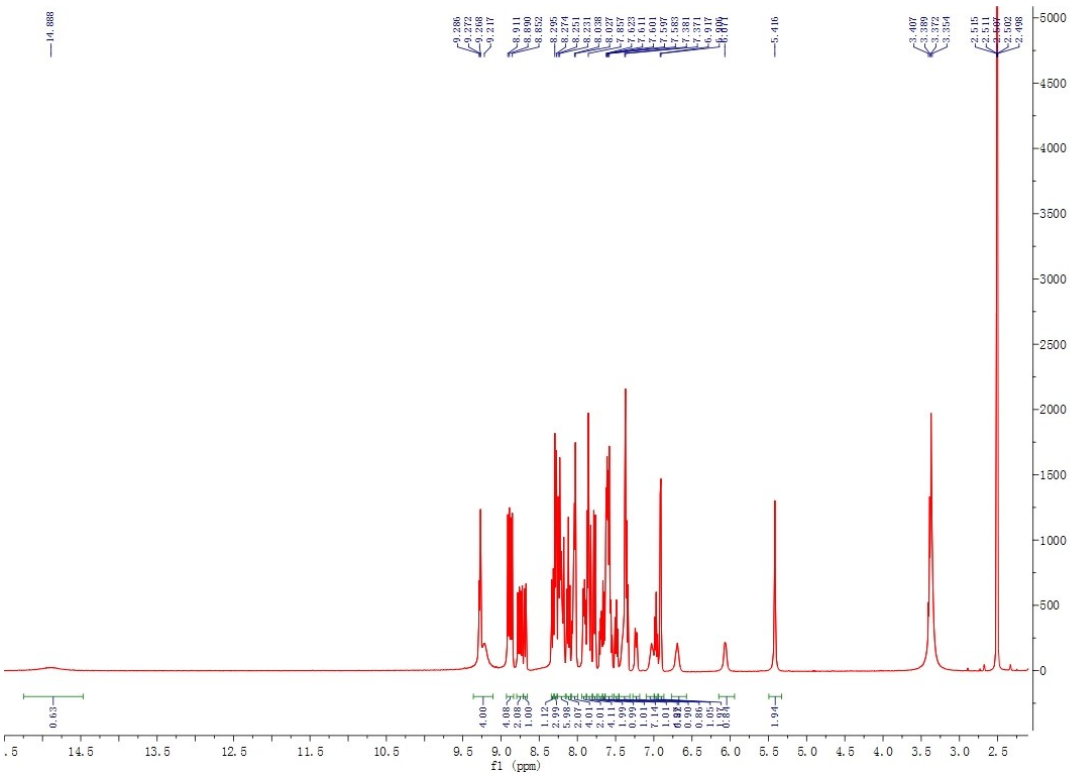

Figure S38. ^{1}H NMR (400 MHz, DMSO-d_6) spectrum of complex **C4**.

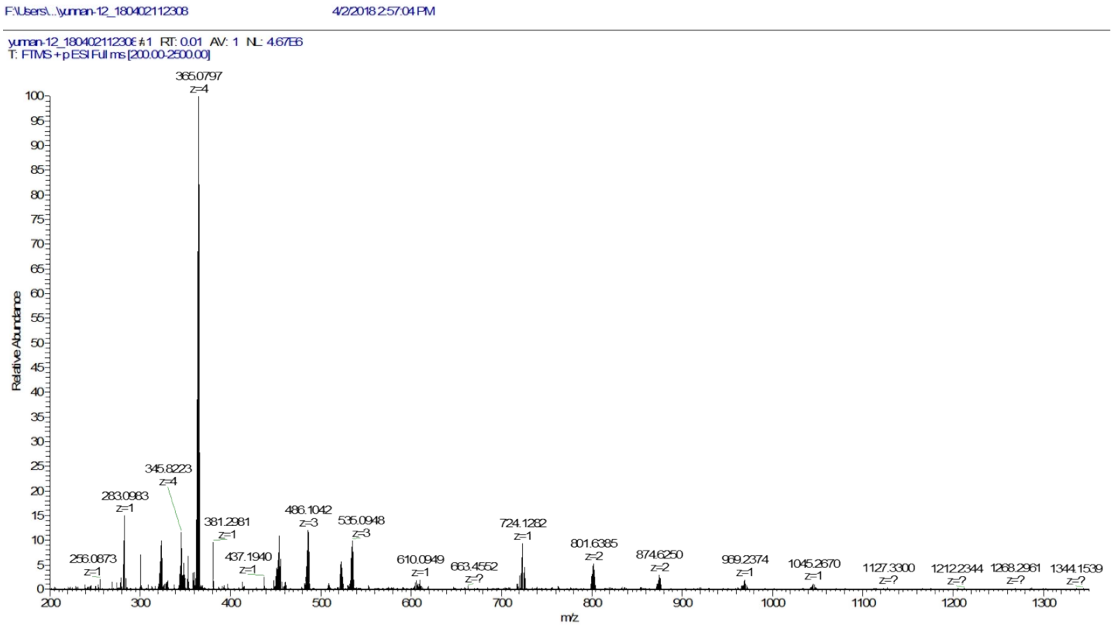

Figure S39. ESI-HRMS of complex **C4**.

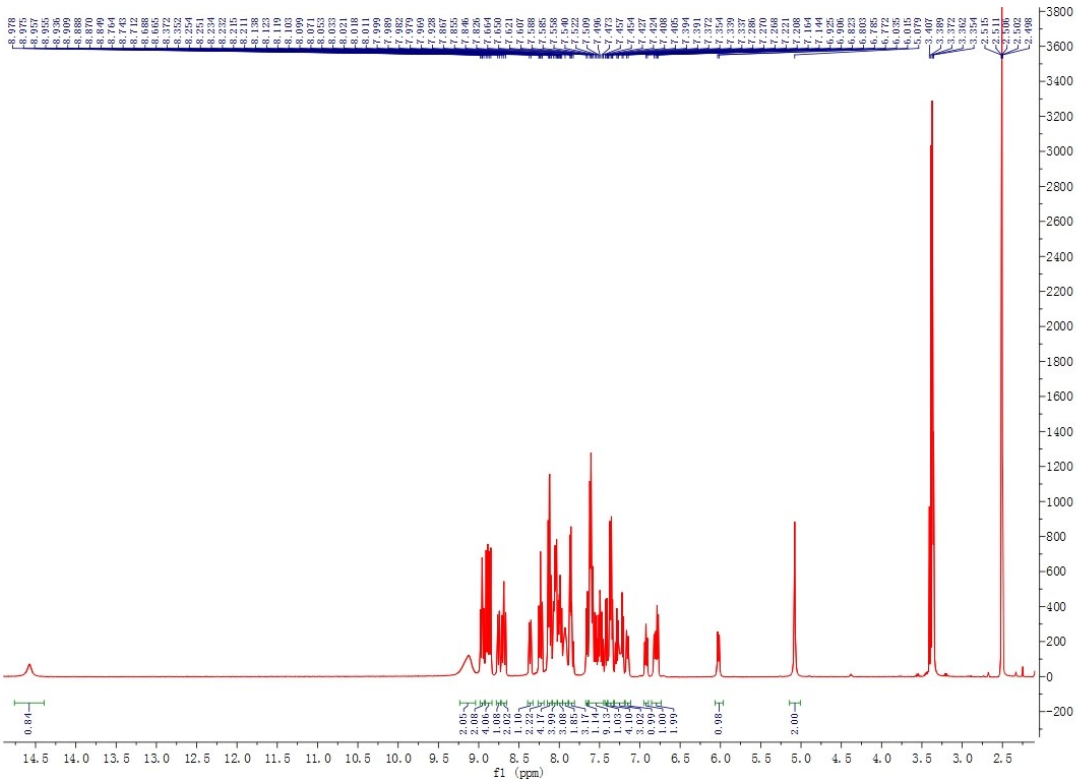

Figure S40. ^{1}H NMR (400 MHz, DMSO-d_6) spectrum of complex **C5**.

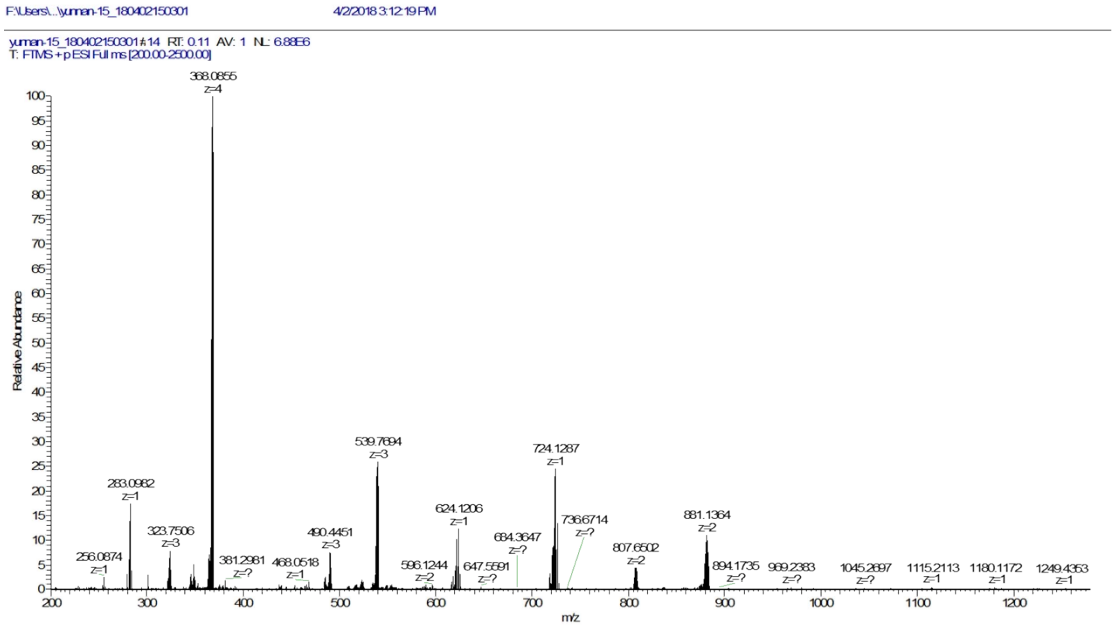

Figure S41. ESI-HRMS of complex **C5**.

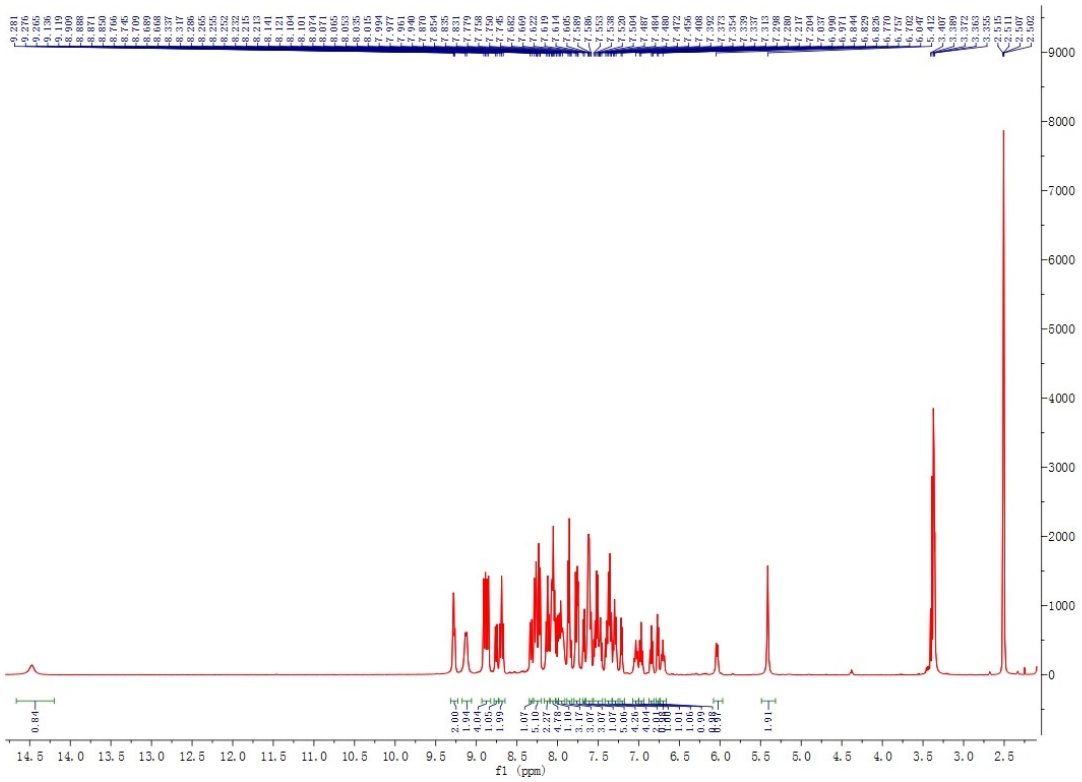

Figure S42. ^{1}H NMR (400 MHz, DMSO-d_6) spectrum of complex **C6**.

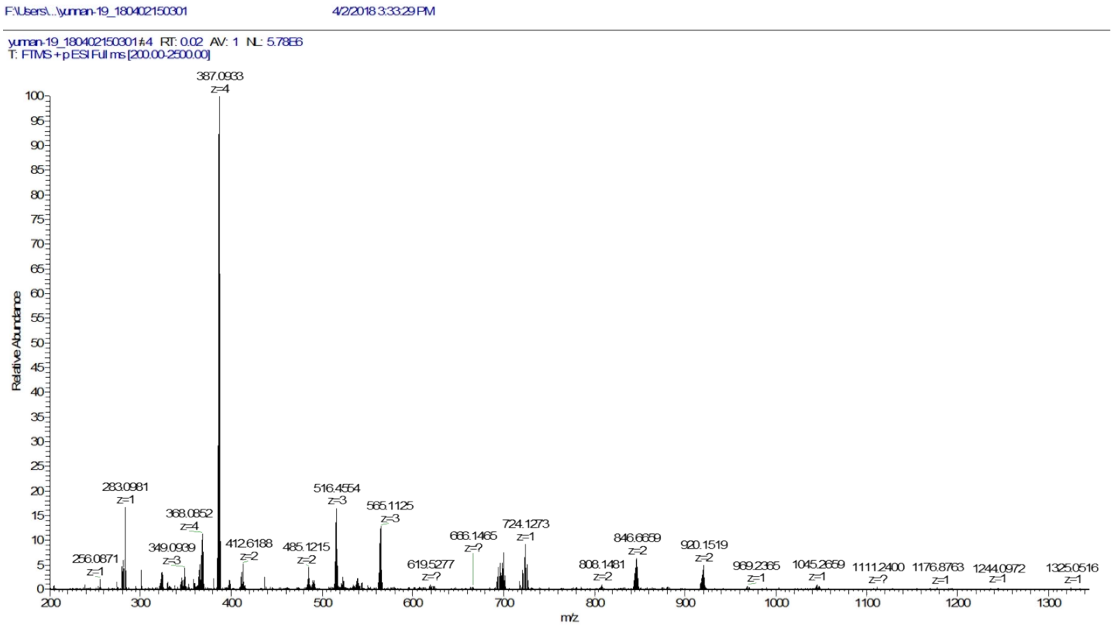

Figure S43. ESI-HRMS of complex **C6**.

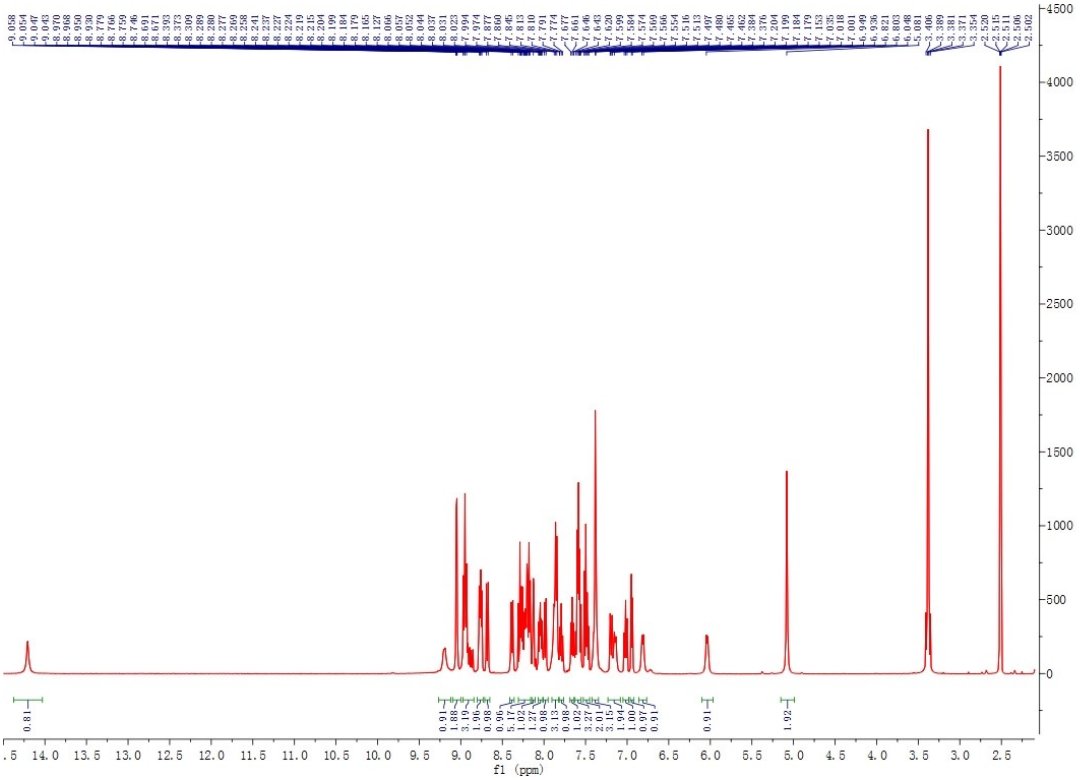

Figure S44. ^{1}H NMR (400 MHz, DMSO-d_6) spectrum of complex **C7**.

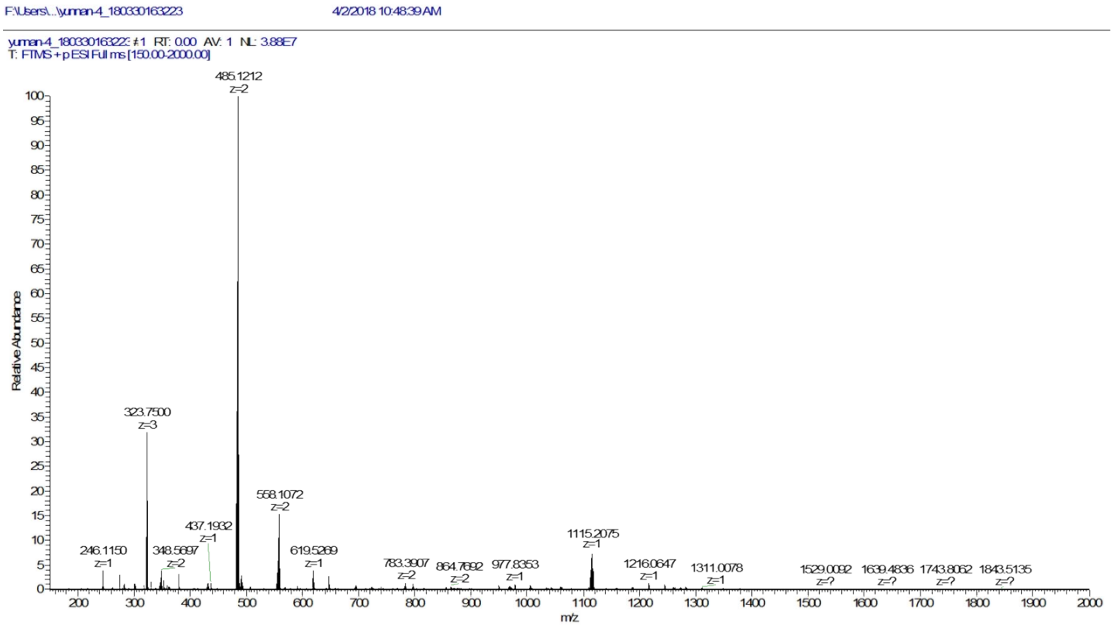

Figure S45. ESI-HRMS of complex **C7**.

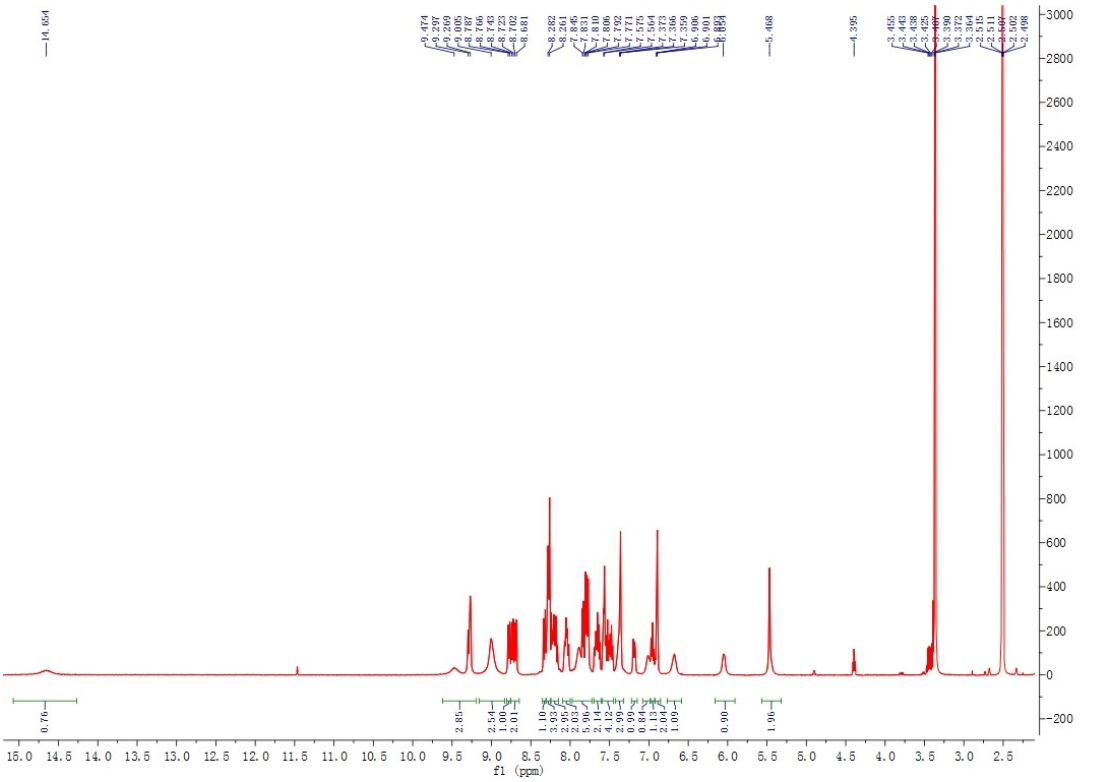

Figure S46. ^{1}H NMR (400 MHz, DMSO-d_6) spectrum of complex **C8**.

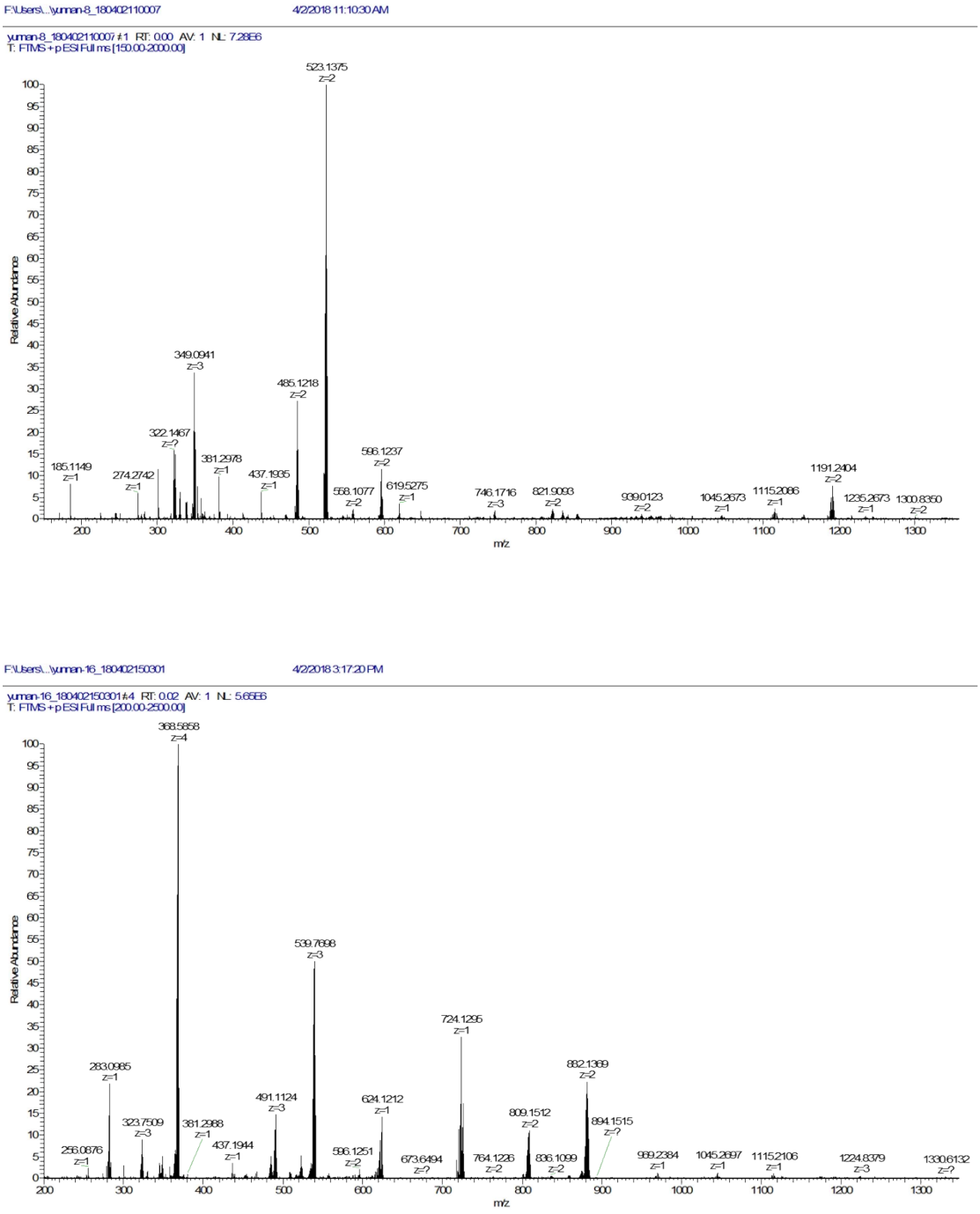

Figure S50. ESI-HRMS of complex **C9**.

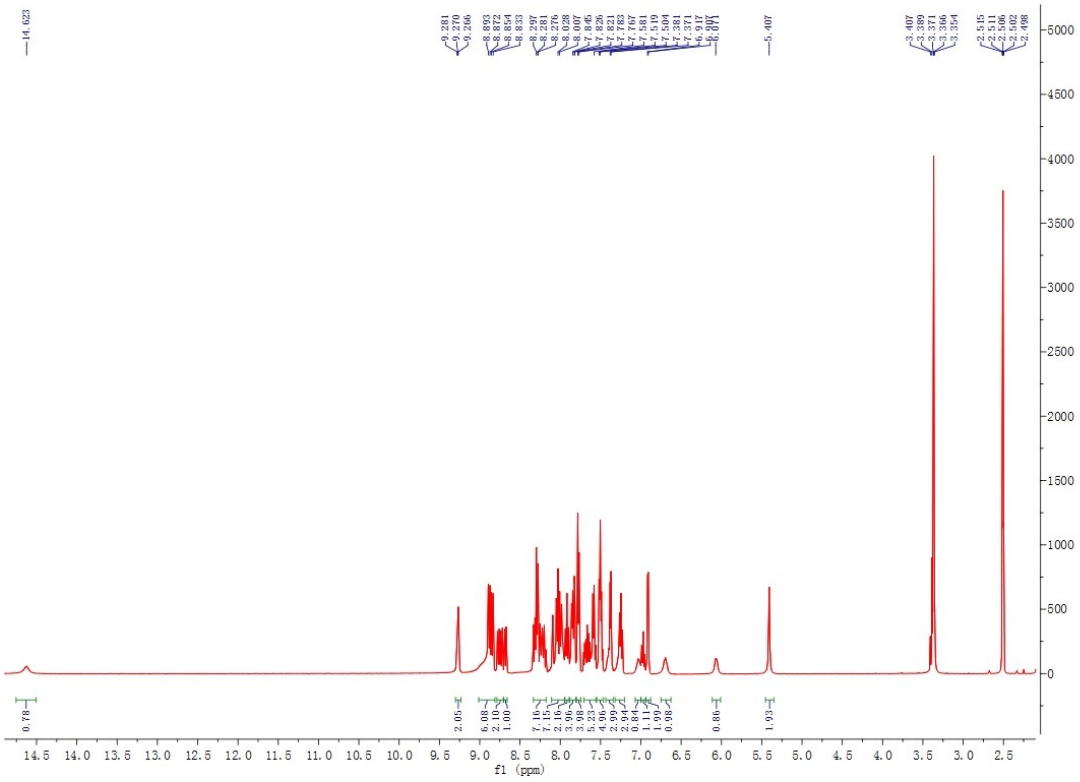

Figure S51. ^{1}H NMR (400 MHz, DMSO-d_6) spectrum of complex **C10**.

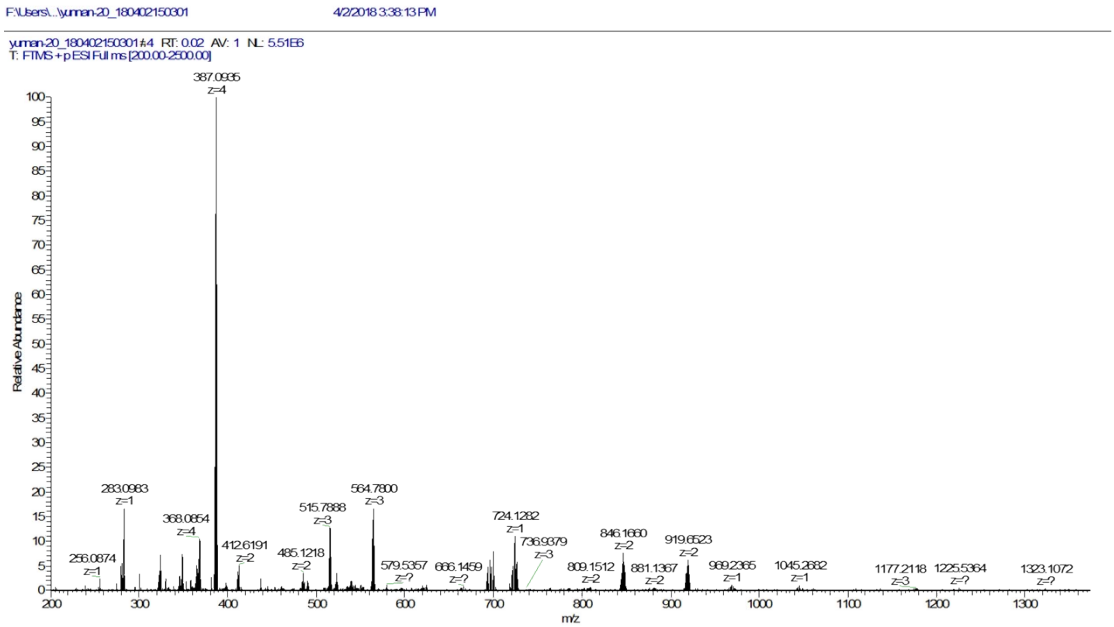

Figure S52. ESI-HRMS of complex **C10**.